

# The $NN \rightarrow NN\pi^+$ Reaction near Threshold in a Chiral Power Counting Approach

Carlos A. da Rocha<sup>a</sup>, Gerald A. Miller<sup>b</sup>, and Ubirajara van Kolck<sup>c,b</sup>

<sup>a</sup> *Instituto de Física Teórica, Universidade Estadual Paulista*

*Rua Pamplona 145, 01405-900 São Paulo-SP, Brazil*

*and*

*Departamento de Desenvolvimento Tecnológico, Universidade São Judas Tadeu*

*Rua Taquari 546, 03166-000 São Paulo-SP, Brazil*

<sup>b</sup> *Department of Physics*

*University of Washington, Box 351560, Seattle, WA 98195-1560*

<sup>c</sup> *Kellogg Radiation Laboratory, 106-38*

*California Institute of Technology, Pasadena, CA 91125*

## Abstract

Power-counting arguments are used to organize the interactions contributing to the  $NN \rightarrow d\pi, pn\pi$  reactions near threshold. We estimate the contributions from the three formally leading mechanisms: the Weinberg-Tomozawa (WT) term, the impulse term, and the  $\Delta$ -excitation mechanism. Sub-leading but potentially large mechanisms, including  $S$ -wave pion-rescattering, the Galilean correction to the WT term, and short-ranged contributions are also examined. The WT term is shown to be numerically the largest, and the other contributions are found to approximately cancel. Similarly to the reaction  $pp \rightarrow pp\pi^0$ , the computed cross sections are considerably smaller than the data. We discuss possible origins of this discrepancy.

NT@UW-98-10  
KRL MAP-236  
IFT - P.058/98

## I. INTRODUCTION

Computations of pion production in nucleon-nucleon ( $NN$ ) collisions near threshold, allow a confrontation of our understanding of  $NN$  interactions with data in a kinematic region for which chiral symmetry, and therefore quantum chromodynamics QCD, could be very important. The reaction  $pp \rightarrow pp\pi^0$  near threshold has attracted much attention in the years since the first IUCF data appeared [1] and has exposed serious disagreements with earlier theoretical calculations [2–5]. The existence of many conflicting models claiming to explain this discrepancy [6–9] calls for a principle to organize the several potentially significant mechanisms of pion production. Chiral Perturbation Theory ( $\chi$ PT) has been applied to mesonic [10,11], one-baryon [12,13], and nuclear [14–21] processes where typical momenta of the order of the pion mass,  $m_\pi$ , allow a systematic expansion of observables in powers of  $m_\pi/M_{QCD}$ , where  $M_{QCD} \sim 1$  GeV. Cohen *et al* [22] have adapted the power counting and applied  $\chi$ PT to near-threshold pion production, where momenta are of order  $\sqrt{m_\pi m_N}$ ,  $m_N$  being the nucleon mass. They estimated leading and next-to-leading contributions, the latter including important short-range contributions, related to the isoscalar components of the potential (and possibly described by  $\sigma$  and  $\omega$  meson exchanges) [6]. Subsequently, van Kolck *et al* [23] showed that next-to-next-to-leading contributions (*e.g.*, from  $\rho - \omega$  meson exchange) are also relevant; data could then be explained within the very large theoretical uncertainties associated with  $S$ -wave pion rescattering and the short-range structure of the nuclear force. Other  $\chi$ PT-inspired calculations have also stressed the importance of understanding rescattering [24] and the effect of loops [24–28]. Since these  $\chi$ PT-inspired calculations include a larger number of contributions than other, model calculations, one concludes that a large theoretical uncertainty plagues all calculations performed to date.

Given such uncertainties, it is natural to examine other channels using the same techniques. Here we are going to discuss  $NN \rightarrow d\pi$  and  $\rightarrow pn\pi$ , which traditionally have been considered better understood than  $pp \rightarrow pp\pi^0$ . We consider energies near threshold where the calculation simplifies, because the pion emerges mostly in an  $S$  wave. We will show that an understanding of these channels is still in the future.

We adopt here the conventional nuclear approach of grouping all  $NN$  interactions generated by mesons of small momentum in a potential, while the contributions associated with energies comparable to  $m_\pi$  are accounted for in a kernel to be evaluated between wavefunctions generated by the potential. Splitting the problem this way, one should still strive to calculate wavefunctions and kernels from the same theory or model, otherwise ambiguities arise from off-shell extrapolations (or equivalently, from nucleon-field redefinitions).  $\chi$ PT is the only known tool for performing this task, and at the same time is consistent with QCD, because its symmetries are treated correctly.  $\chi$ PT is also unique in that it offers the possibility of doing systematic calculations: an expansion in momenta provides a power counting to organize the calculation even though coupling constants are not small.

$\chi$ PT separates interactions in long-range effects calculated explicitly with pion exchange and short-range effects accounted for by contact interactions with an increasing number of derivatives. Parameters not constrained by chiral symmetry depend on details of QCD dynamics, and are at the present unknown functions of QCD parameters. Predictive power is not lost, however, because at any given order in the power counting only a finite number of unknown parameters appear; after they are fitted to a finite set of data, all else can

be predicted at that order. These predictions are called “low-energy theorems”. Since the Lagrangian of  $\chi$ PT is the most general one consistent with QCD symmetries,  $\chi$ PT is a generalization of current algebra.

Unfortunately, the only  $NN$  potential derived in  $\chi$ PT [15] and fitted to low-energy phase shifts [16] produces poor results near the pion production threshold. Attempts to remedy the situation are in progress [20,21]. For the time being we will rely on modern, “realistic” phenomenological potentials which fit  $NN$  data very well. By considering more than one of those, we can estimate the otherwise uncontrolled error stemming from our inconsistent use of potential and kernel. We are going to see that, in contrast to neutral pion production, the error is small in the channel considered here. Because such realistic potentials reproduce low-energy phase shifts with identical long-range tails, they must contain the equivalent to the leading order in the chiral expansion. Although our approach should be considered phenomenological, our leading-order result will be an approximation to a low-energy theorem. At sub-leading orders in the expansion, an apparent ambiguity arises, concerning the correct treatment of the energy transferred in pion rescattering. This can be seen in the conflicting results of estimates of the same kernel [22,24]. This issue is under study [29]; here we will limit ourselves to the most natural prescription that the transferred energy is  $\simeq m_\pi/2$ .

We will concentrate most of our efforts on the kernel. We will discuss a reasonable power counting for pion production that generalizes for  $\pi d$  and  $\pi pn$  channels the discussion of Ref. [22]. In leading order, the new ingredient here is pion rescattering using the Weinberg-Tomozawa (WT) term that dominates isospin-dependent  $\pi N$  scattering. This term does not contribute to the reaction  $pp \rightarrow pp\pi^0$ . In the latter, the leading non-vanishing order consists only of an impulse term (IA), in which a single pion is emitted from a nucleon, and a similar contribution from the delta ( $\Delta$ ). This leading order underpredicts the experimental data by a factor of approximately 5, due to two cancellations not incorporated in our power counting: (*i*) among different regions in coordinate space for each term evaluated between initial and final wavefunctions; and (*ii*) between the total impulse and delta contributions. Oversight (*i*) results from our present inability to treat the potential and the kernel on the same footing. Oversight (*ii*) is somewhat accidental, but actually expected from the fact that, in energy, the pion threshold sits midway between the elastic threshold and the delta pole. The sensitivity of the delta contribution to the realistic potential used is the main source of dependence on the  $NN$  potential of the final result.

As a consequence of the accidentally small leading order, effects which are usually negligible acquire prominence in neutral pion production in the  $pp$  reaction. One effect is isospin-independent pion rescattering.  $\chi$ PT is critically necessary to assess the size of this contribution. First, in principle  $\chi$ PT allows one to determine from  $\pi N$  data not only the momentum- and energy-independent  $2\pi N^\dagger N$  vertex, but also terms which are quadratic in energy and momentum. This is important in view of the fact that in pion production the virtual pion has energy of order  $m_\pi/2$  and the combination of parameters of relevance is thus different from the combination that appears at the  $\pi N$  scattering threshold. There is by now a number of consistent estimates of the relevant parameters to third order [13,30]. An estimate of the uncertainty of this contribution to pion production can be made by using also a lower-order determination [31]. Second,  $\chi$ PT is the only way to account for rescattering as a component of a Feynman diagram without destroying chiral symmetry. There have been attempts to estimate rescattering by simply connecting a nucleon line to a  $\pi N$

amplitude with an arbitrary off-shell extension [7,8]. By considering field redefinitions in the most general chiral Lagrangian, it is easy to show that the off-shell ambiguity in the pion leg is equivalent to a set of short-range  $\pi(N^\dagger N)^2$  interactions, and that an inconsistent treatment of both effects leads to violation of chiral symmetry in a way that is contradictory with QCD [32]. Using  $\chi$ PT, it was found [22,24] that rescattering interferes destructively with the leading-order effects in  $pp \rightarrow pp\pi^0$ . This further interference makes agreement with data more difficult. Although the magnitude of the effect is still being assessed [29], it is certain that the uncertainty stemming from different determinations of the  $\chi$ PT parameters is large [23].

This disagreement between theoretical evaluations and cross-section data for  $pp \rightarrow pp\pi^0$  can be largely removed if  $\sigma$ ,  $\rho$  and other heavy mesons are included [23]. When first suggested [6], it looked as if  $pp \rightarrow pp\pi^0$  was a clear signal of these otherwise elusive mechanisms. Among the first corrections in our power counting, one finds two-pion-exchange loop graphs and  $\pi(N^\dagger N)^2$  counterterms (that behave properly under chiral symmetry). A full  $\chi$ PT calculation requires the calculation of these loops, and although some steps have been taken in this direction [26,28], it is a herculean task that remains to be completed. Even then, it will still require that the counterterms be fitted to some pion production data (say, right at threshold) so that other data (say, the energy dependence close to threshold, or other channels) be predicted. In the case of  $pp \rightarrow pp\pi^0$ , even the most sophisticated phenomenological models have to recourse to such a fit of a short-range counterterm [33]. In any case, after all this one would then be interested in determining whether such counterterms are of natural size, and whether they can be further understood as the result of heavy-meson exchange. In view of all other uncertainties, the authors of Ref. [22] took the point of view that an estimate of this class of sub-leading contributions could more easily be made by modeling them with meson exchange in Z-graphs, following Ref. [6]. It turns out that the counterterms so produced are of natural size, which lends them credence, but that they are not sufficient to achieve agreement with data. In order to study convergence, further meson exchanges (chiefly  $\rho - \omega$ ) that contribute to higher-order counterterms were considered, and shown to be smaller but still relevant [23].

The conclusion of Ref. [23] was that it is possible to describe the  $pp \rightarrow pp\pi^0$  reaction consistently with QCD, reasonable meson exchanges, and realistic potentials, but only within a very large theoretical uncertainty. It is our intention to assess here our theoretical understanding of the  $NN \rightarrow d\pi, \rightarrow pn\pi$  reactions by analyzing the effect of the same microscopic mechanisms.

These reactions have been studied for some time. Conservation of parity, angular momentum, and isospin constrains the possible channels for these reactions. In the case of unbound final nucleons, sufficiently close to threshold the strong  $S$ -wave two-nucleon interaction implies that the most important channels should be those in which the final nucleons have relative orbital angular momentum  $L_{NN} = 0$ . Some of these partial waves are listed in Table I.

Near threshold we expect the pion, too, to be in an  $S$ -wave, and the cross sections to be nearly isotropic, with [34]

$$\frac{d\sigma}{d\Omega}(pp \rightarrow pn\pi^+) = \frac{1}{4} \left( |a_1|^2 + \frac{1}{3}|b_0|^2 \right) + \dots, \quad (1)$$

TABLE I. Partial-wave amplitudes for the  $NN \rightarrow NN\pi$  reactions that can contribute to the isotropic cross section right at threshold with an  $L_{NN} = 0$  final state.  $L_{\pi(NN)}$  denotes the pion angular momentum.

Element	$NN$ Initial state	$NN$ final state	$L_{\pi(NN)}$
$a_0$	$^1S_0$	$^3S_1$	1
$a_1$	$^3P_1$	$^3S_1$	0
$a_2$	$^1D_2$	$^3S_1$	1
$b_0$	$^3P_0$	$^1S_0$	0

$$\frac{d\sigma}{d\Omega}(pp \rightarrow d\pi^+) = \frac{1}{4}|a'_1|^2 + \dots, \quad (2)$$

$$\frac{d\sigma}{d\Omega}(pp \rightarrow pp\pi^0) = \frac{1}{12}|b_0|^2 + \dots \quad (3)$$

Here  $a_1$  and  $a'_1$  have quite different magnitudes due to the different wavefunctions; in the case of the deuteron final state the effect of the  $D$  wave is also important, and it is incorporated in the following. The cross section for  $np \rightarrow d\pi^0$  is related to that of  $pp \rightarrow pn\pi^+$  by isospin considerations. There is a relative factor 2 from  $pp$  being pure isospin  $I = 1$  and  $np$  having  $I = 1$  and  $I = 0$  in equal probabilities; and there are Coulomb effects. The total cross-section for the deuteron channels is function of  $\eta = q/m_\pi$  where  $q$  is the maximum pion momentum. It is well-known [35,36] that sufficiently close to threshold the cross-section for  $np \rightarrow d\pi^0$  is

$$\sigma_{np} = \frac{\alpha}{2}\eta + \mathcal{O}(\eta^3), \quad (4)$$

while for  $pp \rightarrow d\pi^+$  it is

$$\sigma_{pp} = \alpha C_0^2 \eta + \mathcal{O}(\eta^3). \quad (5)$$

Here  $\alpha$  is a constant which depends on the strong interactions that produce the pion and  $C_0(\eta)$  is a Coulomb factor arising mostly from the pion-deuteron electromagnetic interaction. If the experimental data for  $pp \rightarrow d\pi^+$  are corrected for these electromagnetic effects, then both reactions near threshold can be viewed as a determination of the single constant  $\alpha$ . The threshold behavior of the reaction  $pp \rightarrow pn\pi^+$  was estimated by Gell-Mann and Watson [35], who predicted an energy dependence  $\sigma \propto \eta^4$  under the approximation of zero-range nuclear forces.

Early theoretical analyses of the reaction  $pp \rightarrow d\pi^+$ , like in ours, split it into a kernel—where the two-nucleon system emits the pion—and effects of initial- and final-state interactions—taken into account by using deuteron and scattering wave functions that satisfy the Schrödinger equation with a given  $NN$  potential. The numerical results of the early analyses [2] were that this reaction is dominated by the Weinberg-Tomozawa (WT) term (Fig. 1b). The main competitor process was thought to be the impulse term (IA) (Fig. 1a). The early estimate of this IA gave a small contribution [2] due to a cancellation in the matrix

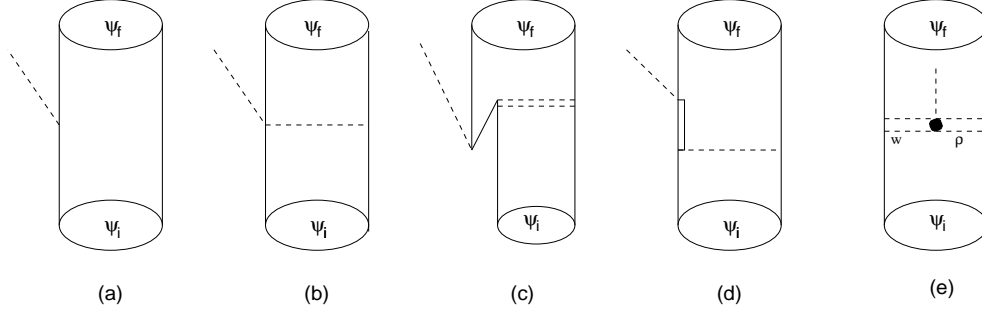


FIG. 1. Various contributions to the  $pp \rightarrow d\pi^+, pn\pi^+$  reactions. A single (double) solid line stands for a nucleon (delta) and a single (double) dashed line represents a pion (sigma, omega, rho);  $\Psi_i$  ( $\Psi_f$ ) is the wave function for the initial (final) state.

elements between the  $S$  and  $D$  waves of the deuteron final state. It was believed that the WT term alone could account for the essential features of the data.

With the advent of accelerators capable of producing intense high-quality beams of protons with GeV energies and very precise detecting systems, good and accurate data for  $np \rightarrow d\pi^0$  [37],  $pp \rightarrow d\pi^+$  [38,39], and  $pp \rightarrow pn\pi^+$  [40,41] near threshold became available. For the deuteron channels, the new data confirm the threshold behavior (4) [37], and show that the theoretical calculations started by Koltun and Reitan were in the right direction. More recent calculations of the WT and IA mechanisms [42,25], however, indicated that their strength might not be sufficient to explain the new data. As for the unbound final state, the recent measurements in the Indiana Cooler [41] give

$$|a_1|^2 \propto \eta^{3.2}. \quad (6)$$

A calculation [43] using IA, on-shell pion rescattering, and  $\sigma, \omega$  Z-graphs finds good agreement with data in all  $pp\pi^0$ ,  $pn\pi^+$ , and  $d\pi^+$  channels with a soft  $\pi N$  form factor.

Our motivation here is to examine what a chiral power counting suggests for the pion production in the  $pp \rightarrow d\pi^+$  and  $pp \rightarrow pn\pi^+$  reactions near threshold. For the  $d\pi^+$  reaction, we will compute  $\sigma_{pp}$  but will disregard the Coulomb interaction in both the initial state—which is not so important due to the not-so-small initial energy—and final state. This means we do not calculate  $C_0(\eta)$ , and can only compare with Coulomb-corrected  $pp$  data. We will see that  $\sigma_{pp}$  is indeed approximately linear with  $\eta$  at threshold, so our result can be considered a calculation of  $\alpha$  in Eq. (5). Alternatively, it is a calculation of  $2\sigma_{np}$ . For the  $pn\pi^+$  final state, we will also disregard the Coulomb interaction and see that our cross section has an energy dependence similar to the data. Moreover, we will show that the WT term is indeed the dominant one, not only for the  ${}^3S_1$   $pn\pi^+$  final state but also for the deuteron channel, which is consistent with the early analyses for this final state. The IA term is smaller than WT because of cancellations between different regions in coordinate space, and between the  $S$  and  $D$  waves of the deuteron final state. The same cancellations affect the contribution from an explicit  $\Delta$  in the intermediate state (Fig. 1d), more so in the  $d\pi^+$  channel than in the  $pn\pi^+$  channel. The relative smallness of this term here reduces the effects of using different  $NN$  potentials compared to the  $pp \rightarrow pp\pi^0$  reaction. However the delta contribution is affected by a number of uncertainties. We include also the same

sub-leading terms that proved important in the  $pp \rightarrow pp\pi^0$  reaction: isospin-independent rescattering (ST, Fig. 1b), and heavy meson exchange simulating short-range mechanisms ( $\sigma, \omega$  and  $\rho - \omega$ , Fig. 1c,e). The sub-leading Galilean correction to the WT term (GC) is included as well. These contributions are all relatively small. We will see that, if we neglect the uncertain  $\Delta$  contributions, each of the the cross-sections is underestimated by a factor of  $\sim 2$ .

In Section II we discuss the power counting and the chiral Lagrangian. In Section III the kernel is obtained. In Section IV the calculation of the cross-sections is outlined; some technical details are relegated to an Appendix. Section V describes our input and discusses our results. An outlook is presented in Section VI.

## II. IMPLEMENTING $\chi$ PT

Near threshold for pion production the total energy of the two colliding nucleons is of order  $2m_N + m_\pi$ , so that the center-of-mass initial kinetic energy of each nucleon is  $m_\pi/2$ . This energy is smaller than the nucleon mass, so we can use a non-relativistic framework. The nonrelativistic kinetic energy formula holds; the mass  $2m_N$  plays no dynamical role, and the typical momentum of real and virtual particles involved in this process is  $p_{\text{typ}} \sim \sqrt{m_N m_\pi}$ . This requires some adaptation of the usual effective theory ideas which have been developed for momenta typical of most nuclear systems,  $Q \sim m_\pi$ . Because the mass difference between the delta isobar and the nucleon,  $\delta = m_\Delta - m_N$ , is numerically of order of the typical excitation energy we are interested in,  $m_\pi$ , the  $\Delta$  must be included explicitly as a degree of freedom in the Lagrangian. On the other hand,  $\sqrt{m_N m_\pi}$  is smaller than the characteristic mass scale of QCD,  $M_{QCD} \sim 1\text{GeV}$ , at least in the chiral limit  $m_\pi \rightarrow 0$ , so that the contribution of other states (the Roper, the  $\rho$  meson, *etc.*) can be buried in short-range interactions.

We thus seek a theory of non-relativistic nucleons and deltas interacting with pions that is consistent with the symmetries of QCD.  $\chi$ PT is implemented via the most general Lagrangian involving these degrees of freedom aided by power-counting arguments. The seminal idea was contained in a paper by Weinberg [10]. This idea was developed systematically for interactions of mesons [11] and for interactions of mesons with a baryon [12,13]. The generalization of these techniques to describe properties of more than one baryon was also due to Weinberg [14] and was carried out in detail in Ref. [15–17]; see also Refs. [18,19,21].

When dealing with typical momenta of order  $Q \sim m_\pi$ , the usual power counting suggests that we order terms in the chiral Lagrangian according to the “index”  $\Delta = d + \frac{f}{2} - 2$ , where  $d$  is the sum of the number of derivatives, the number of powers of  $m_\pi$ , and the number of powers of  $\delta$ ; and  $f$  is the number of fermion field operators. In the following we will consider interactions with  $\Delta$  up to 4.

The Lagrangian with  $\Delta = 0$  for each interaction [10–14,16,17] is

$$\begin{aligned} \mathcal{L}^{(0)} = & \frac{1}{2}(\dot{\boldsymbol{\pi}}^2 - (\vec{\nabla}\boldsymbol{\pi})^2) - \frac{1}{2}m_\pi^2\boldsymbol{\pi}^2 \\ & + N^\dagger[i\partial_0 - \frac{1}{4f_\pi^2}\boldsymbol{\tau} \cdot (\boldsymbol{\pi} \times \dot{\boldsymbol{\pi}})]N + \frac{g_A}{2f_\pi}N^\dagger(\boldsymbol{\tau} \cdot \vec{\sigma} \cdot \vec{\nabla}\boldsymbol{\pi})N \end{aligned}$$

$$+\Delta^\dagger[i\partial_0 - \delta]\Delta + \frac{h_A}{2f_\pi}[N^\dagger(\mathbf{T} \cdot \vec{S} \cdot \vec{\nabla}\boldsymbol{\pi})\Delta + h.c.] + \dots, \quad (7)$$

where  $f_\pi = 93$  MeV is the pion decay constant,  $\delta = m_\Delta - m_N$  is the isobar-nucleon mass difference,  $g_A$  is the axial-vector coupling of the nucleon,  $h_A$  is the  $\Delta N\pi$  coupling, and  $\vec{S}$  and  $\mathbf{T}$  are the transition spin and isospin matrices, normalized such that

$$S_i S_j^+ = \frac{1}{3}(2\delta_{ij} - i\varepsilon_{ijk}\sigma_k) \quad (8)$$

$$T_a T_b^+ = \frac{1}{3}(2\delta_{ab} - i\varepsilon_{abc}\tau_c). \quad (9)$$

Notice that we defined the fields  $N$  and  $\Delta$  in such a way that there is no factor of  $\exp(-im_N t)$  in their time evolution. Hence  $m_N$  does not appear explicitly at this index, corresponding to static baryons. We also wrote  $\mathcal{L}^{(0)}$  in the rest frame of the baryons, which is the natural choice. (Galilean invariance will be ensured by including terms with additional derivatives.) Chiral symmetry determines the coefficient of the so-called Weinberg-Tomozawa term ( $N^\dagger \boldsymbol{\tau} \cdot (\boldsymbol{\pi} \times \dot{\boldsymbol{\pi}})N$ ) but not of the single-pion interactions ( $g_A, h_A$ ).

The Lagrangian with  $\Delta = 1$  is [12,13,16,17],

$$\begin{aligned} \mathcal{L}^{(1)} = & \frac{1}{2m_N}[N^\dagger \vec{\nabla}^2 N + \frac{1}{4f_\pi^2}(iN^\dagger \boldsymbol{\tau} \cdot (\boldsymbol{\pi} \times \vec{\nabla}\boldsymbol{\pi}) \cdot \vec{\nabla}N + h.c.)] \\ & + \frac{1}{f_\pi^2}N^\dagger[(c_2 + c_3 - \frac{g_A^2}{8m_N})\dot{\boldsymbol{\pi}}^2 - c_3(\vec{\nabla}\boldsymbol{\pi})^2 - 2c_1 m_\pi^2 \boldsymbol{\pi}^2 - \frac{1}{2}(c_4 + \frac{1}{4m_N})\varepsilon_{ijk}\varepsilon_{abc}\sigma_k\tau_c\partial_i\pi_a\partial_j\pi_b]N \\ & + \frac{\delta m_N}{2}N^\dagger[\tau_3 - \frac{1}{2f_\pi^2}\pi_3\boldsymbol{\pi} \cdot \boldsymbol{\tau}]N + \frac{1}{2m_N}\Delta^\dagger[\vec{\nabla}^2 + \dots]\Delta \\ & - \frac{g_A}{4m_N f_\pi}[iN^\dagger \boldsymbol{\tau} \cdot \dot{\boldsymbol{\pi}}\vec{\sigma} \cdot \vec{\nabla}N + h.c.] - \frac{h_A}{2m_N f_\pi}[iN^\dagger \mathbf{T} \cdot \dot{\boldsymbol{\pi}}\vec{S} \cdot \vec{\nabla}\Delta + h.c.] \\ & - \frac{d_1}{f_\pi}N^\dagger(\boldsymbol{\tau} \cdot \vec{\sigma} \cdot \vec{\nabla}\boldsymbol{\pi})N N^\dagger N - \frac{d_2}{2f_\pi}\varepsilon_{ijk}\varepsilon_{abc}\partial_i\pi_a N^\dagger\sigma_j\tau_b N N^\dagger\sigma_k\tau_c N + \dots, \quad (10) \end{aligned}$$

where the  $c_i$ 's are coefficients of  $\mathcal{O}(1/M)$ ,  $\delta m_N \sim m_d - m_u$  is the quark mass difference contribution to the neutron-proton mass difference, and the  $d_i$ 's are coefficients of  $\mathcal{O}(1/f_\pi^2 M)$ . These seven numbers are not fixed by chiral symmetry, but it is important to point out that Galilean invariance requires that the other coefficients explicitly shown above be related to those appearing in  $\mathcal{L}^{(0)}$ . This in particular fixes the strength of the single-pion interactions in terms of the lowest-order coefficients  $g_A$  and  $h_A$ , and of the common mass  $m_N$ .

The Lagrangian with  $\Delta = 2$  is

$$\begin{aligned} \mathcal{L}^{(2)} = & \frac{d'_1 + e_1}{2m_N f_\pi}[iN^\dagger \boldsymbol{\tau} \cdot \dot{\boldsymbol{\pi}}\vec{\sigma} \cdot \vec{\nabla}N N^\dagger N + h.c.] \\ & - \frac{e_1}{2m_N f_\pi}[iN^\dagger \boldsymbol{\tau} \cdot \dot{\boldsymbol{\pi}}\vec{\sigma}N \cdot N^\dagger \vec{\nabla}N + h.c.] \\ & + \frac{e_2}{2m_N f_\pi}[N^\dagger \boldsymbol{\tau} \cdot \dot{\boldsymbol{\pi}}\vec{\sigma} \times \vec{\nabla}N \cdot N^\dagger \vec{\sigma}N + h.c.] + \dots, \quad (11) \end{aligned}$$

where the  $e_i$ 's are other coefficients of  $\mathcal{O}(1/f_\pi^2 M)$ .



Among the Lagrangians with higher indices, we find

$$\mathcal{L}^{(4)} = \frac{g}{2m_N f_\pi} [iN^\dagger \boldsymbol{\tau} \cdot \boldsymbol{\pi} \boldsymbol{\sigma} \cdot \vec{\nabla} \vec{\nabla} N \cdot N^\dagger \vec{\nabla} N + h.c.] + \dots, \quad (12)$$

where  $g$  is a coefficient of  $\mathcal{O}(1/f_\pi^2 M^3)$ .

The two nucleons in the  $NN \rightarrow NN\pi$  reaction can interact repeatedly by the exchange of mesons of momenta  $Q \sim m_\pi$  before and after the emission of the pion. We account for this through the iteration of a potential, which produces initial and final wavefunctions that differ from the free ones. The emission of the pion, on the other hand, involves the larger momentum  $p_{\text{typ}} \sim \sqrt{m_N m_\pi}$ . The sub-diagrams that involve such typical momentum form the kernel of “irreducible diagrams”, which is evaluated between wavefunctions.

The unusually high momentum in the kernel requires modification in the usual power counting. While in the usual power counting energy and momenta are counted as equal, here energies are  $\sim m_\pi$  but momenta  $\sim \sqrt{m_N m_\pi}$ . This changes the usual correspondence between index and order.

The leading nucleon propagator, for example, includes both the static term in (7) and the kinetic term in (10) at the same order in power counting for pion production, contrary to the situation in  $\chi$ PT applied to one-baryon systems. The nucleon propagator then is  $\sim 1/m_\pi$ . Relativistic corrections  $p^4/8m_N^3 + \dots$  are relatively smaller by  $\sim m_\pi/m_N$  and can be considered higher-order insertions. Note that this is completely consistent with our decomposition of the full amplitude into a kernel and wavefunctions obtained from a Schrödinger equation, and, contrary to what is stated in Ref. [27], does *not* imply the need of a relativistic framework. The delta propagator differs from the nucleon by the presence of the mass difference  $\delta \sim 2m_\pi$ . As pointed out first in Ref. [22], the delta propagator is then actually  $\sim -1/m_\pi$  and tends to interfere destructively with the nucleon contributions to the kernel. The pion propagator, on the other hand, is  $\sim 1/m_\pi m_N$ . In interactions, each time derivative is associated with a factor of  $m_\pi$ , while a space derivative a factor of  $\sqrt{m_N m_\pi}$ . Finally, a loop brings a  $(m_N m_\pi)^{3/2} m_\pi / (4\pi)^2$ .

A detailed analyses of various contributions can found in Ref. [22]. The new elements here are those associated with the isospin-dependent WT pion rescattering. The order of the WT contribution is evaluated as follows. The term proportional to  $\partial_0 \boldsymbol{\pi}$  of Eq. (7) yields an explicit factor of  $m_\pi/f_\pi^2$ ; the pion-nucleon interaction provides a factor of  $\sqrt{m_\pi m_N}/f_\pi$ , and the pion propagator  $(m_\pi m_N)^{-1}$ . The total net result is of order  $\mathcal{O}(f_\pi^{-3} \sqrt{m_\pi/M})$ , which is the same order of the impulse approximation and the delta contribution [22]. Therefore due to power counting arguments, we expect that contribution of WT, IA, and  $\Delta$  terms to have the same importance; they constitute our leading order. We will also include other terms which are of order  $m_\pi/M$  or higher relative to the leading one: the isospin-independent pion rescattering (SG), the Galilean correction to the WT term (GC), and contact terms, modeled by the heavy meson exchange ( $\sigma$ ,  $\omega$  and  $\rho - \omega$ ).

### III. THE KERNEL

We now obtain the explicit forms of the various contributions by evaluating the most important irreducible diagrams in momentum space. Our notation is as follows:  $\omega_q^2 =$

$\vec{q}^2 + m_\pi^2$  is the energy of the (on-shell) pion produced with momentum  $\vec{q}$  in the center of mass;  $\vec{p}$  ( $\vec{p}'$ ) is the center-of-mass momentum of the incoming (outgoing) nucleon labeled “1” (those of nucleon “2” are opposite);  $\vec{k} = \vec{p} - \vec{p}'$  ( $k^0 = m_\pi/2$ ) is the momentum (energy) transferred;  $\omega_k^2 = \vec{k}^2 + m_\pi^2$ ;  $\vec{P} = \vec{p} + \vec{p}'$ ;  $\vec{\sigma}^{(i)}$  is the spin of proton  $i$ ;  $\vec{\Sigma}_a = \vec{\sigma}^{(1)}\tau_a^{(1)} - \vec{\sigma}^{(2)}\tau_a^{(2)}$  where  $a$  is the isospin of emitted pion; and  $T(\vec{k}) \equiv \vec{\sigma}^{(1)} \cdot \vec{k} \vec{\sigma}^{(2)} \cdot \vec{k}$ . We define the  $T$ -matrix in terms of the  $S$ -matrix via  $S = 1 + iT$ .

According to the previous discussion, we expect the leading contributions to arise from the diagrams in Figs. 1a,b, and d. In the case of the Weinberg-Tomozawa diagram (Fig. 1b), we get

$$T_a^{WT} = -\frac{g_A}{4f_\pi^3} \epsilon_{abc} \tau_b^{(1)} \tau_c^{(2)} \frac{\omega_q + k^0}{\omega_k^2 - (k^0)^2} \vec{S} \cdot \vec{k}. \quad (13)$$

The Galilean correction to WT contribution is smaller by a factor of  $m_\pi/M$  and is given by

$$T_a^{GC} = -\frac{g_A}{8m_N f_\pi^3} \epsilon_{abc} \tau_b^{(1)} \tau_c^{(2)} \frac{1}{\omega_k^2 - (k^0)^2} \vec{k} \cdot \vec{P} \vec{S} \cdot \vec{k}. \quad (14)$$

The impulse term (Fig. 1a) is discussed in detail in [22]. The principle of irreducibility says that we have to redraw this diagram. Since the outgoing pion carries an energy of the order of the pion mass, the energies of the  $NN$  intermediate state before and after pion emission differ by  $\sim m_\pi$ . Therefore both of the intermediate states cannot simultaneously be within  $\sim m_\pi^2/m_N$  of being on-shell: at least one intermediate state, before or after emission, is off shell by  $\sim m_\pi$ . This single, relatively-high-momentum ( $\sim \sqrt{m_\pi m_N}$ ) pion exchange must therefore be included in the irreducible class of operators for our process (unlike the usual case). All other initial- and final-state interactions will be considered reducible and included in the wave functions. Therefore, in the case of pion exchange with a nucleon in the intermediate state we get

$$T_a^{IA} = \frac{ig_A^3}{8m_N f_\pi^3} \frac{1}{\omega_k^2 - (k^0)^2} \left[ \vec{\Sigma}_a \cdot \vec{p}' T(\vec{k}) - T(\vec{k}) \vec{\Sigma}_a \cdot \vec{p} \right], \quad (15)$$

which is listed for comparative purposes only. We will actually calculate the impulse approximation directly from Eq.(6) in Ref. [22], in the same fashion as done by Koltun and Reitan [2].

Recoil corrections are expected to be smaller by a factor of  $m_\pi/M$ . Since the impulse contribution will prove to be small, we can ignore the recoil contributions in this first approach.

The  $\Delta$  contribution (Fig. 1d) to the kernel is given by

$$T_a^\Delta = \frac{-ig_A h_A^2}{18m_N f_\pi^3} \frac{1}{\omega_k^2 - (k^0)^2} \frac{\omega_q}{\delta^2 - \omega_q^2} \times \left[ \left( \vec{k}^2 \omega_q - \vec{k} \cdot \vec{P} \delta \right) \vec{\Sigma}_a \cdot \vec{k} + \frac{i}{2} \omega_q \left( \tau_a^{(1)} \vec{\sigma}^{(1)} \cdot \vec{k} \vec{\sigma}^{(2)} \cdot (\vec{P} \times \vec{k}) - \tau_a^{(2)} \vec{\sigma}^{(1)} \cdot (\vec{P} \times \vec{k}) \vec{\sigma}^{(2)} \cdot \vec{k} \right) \right] + i\epsilon_{abc} \tau_b^{(1)} \tau_c^{(2)} \left[ \left( \omega_q \vec{k} \cdot \vec{P} - \delta \vec{k}^2 \right) \vec{S} \cdot \vec{k} - \frac{i}{4} \delta \left( \vec{\sigma}^{(1)} \cdot \vec{k} \vec{\sigma}^{(2)} \cdot (\vec{P} \times \vec{k}) + \vec{\sigma}^{(1)} \cdot (\vec{P} \times \vec{k}) \vec{\sigma}^{(2)} \cdot \vec{k} \right) \right]. \quad (16)$$

Results similar to Eqs. (15) and (16) follow for shorter-range terms where the two nucleons exchange a heavier meson rather than a pion. In the case of a nucleon intermediate state, such a contribution is automatically included in the potential. In any reasonable model, the contributions from a delta intermediate state turn out to be smaller than those in diagram of Fig. 1d. For example, they could arise from  $a_1$  exchange, but then the relatively high  $a_1$  mass suppresses this contribution; the contribution from the  $\rho$  which is formally of higher-order is likely to be more important. Since, as we are going to see, the delta contribution from pion exchange is not large, we will not go into such detailed analysis for the purpose of estimating the effect of the  $\Delta$ : we use Eq.(16). We will further discuss the uncertainties related to the delta contribution below.

There are other corrections of order  $m_\pi/M$  compared to the leading terms. Fig. 1b represents also isospin-independent rescattering:

$$T_a^{ST} = i \frac{g_A}{f_\pi^3} \frac{1}{\omega_k^2 - (k^0)^2} \left\{ \left[ \left( c_2 + c_3 - \frac{g_A^2}{8m_N} \right) k^0 \omega_q - 2c_1 m_\pi^2 \right] \vec{\Sigma}_a \cdot \vec{k} - \frac{\delta m_N}{8} \left[ \delta_{3a} \vec{\tau}^{(1)} \cdot \vec{\tau}^{(2)} \left( \vec{\sigma}^{(1)} - \vec{\sigma}^{(2)} \right) + \vec{\sigma}^{(1)} \tau_3^{(1)} \tau_a^{(2)} - \vec{\sigma}^{(2)} \tau_a^{(1)} \tau_3^{(2)} \right] \cdot \vec{k} \right\}. \quad (17)$$

The short-range mechanisms provided by the  $\Delta = 2, 3, 4$  Lagrangians involve several unknown constants. Chiral symmetry tells us nothing about the strength of these coefficients. We can use data to determine some of them. Alternatively, we can use a model to determine these coefficients and then try to explain the experimental results. Here we use the mechanism first proposed by Lee and Riska [6] and by Horowitz *et al* [7], where the short-range interaction is supposed to originate from Z-graphs with  $\sigma$  and  $\omega$  exchanges, as shown in Fig. 1c. In this case,

$$T_a^{\sigma, \omega} = -\frac{i g_A}{4f_\pi m_N^2} \omega_q \left[ \left( \frac{g_\sigma^2}{\vec{k}^2 + m_\sigma^2} + \frac{g_\omega^2}{\vec{k}^2 + m_\omega^2} \right) \vec{\Sigma}_a \cdot \vec{P} - i \frac{g_\omega^2 (1 + C_\omega)}{\vec{k}^2 + m_\omega^2} \vec{\sigma}^{(1)} \times \vec{\sigma}^{(2)} \cdot \vec{k} \left( \tau_a^{(1)} + \tau_a^{(2)} \right) \right], \quad (18)$$

where  $m_\sigma$  ( $m_\omega$ ) and  $g_\sigma$  ( $g_\omega$ ) are the mass and the vector coupling to nucleons of the  $\sigma$  ( $\omega$ ) meson, and  $C_\omega$  denotes the ratio of tensor to vector coupling for the  $\omega$  meson. In the case of  $pp \rightarrow pp\pi^0$ , the contribution due to  $\rho - \omega$  exchange (Fig. 1e) is not negligible [23], so we also include it here in order to get an estimate of the convergence of our expansion. This contribution leads to

$$T_a^{\rho, \omega} = -\frac{i g_\rho g_\omega g_{\pi\rho\omega}}{4m_N^2} \frac{\omega_q}{m_\omega} \left( \frac{g_\rho^2}{\vec{k}^2 + m_\rho^2} \cdot \frac{g_\omega^2}{\vec{k}^2 + m_\omega^2} \right) \left\{ (2 + C_\rho + C_\omega) \left( \vec{k}^2 \vec{\Sigma}_a \cdot \vec{P} - \vec{k} \cdot \vec{P} \vec{\Sigma}_a \cdot \vec{k} \right) - i (1 + C_\rho) (1 + C_\omega) \vec{k}^2 \vec{\sigma}^{(1)} \times \vec{\sigma}^{(2)} \cdot \vec{k} \left( \tau_a^{(1)} + \tau_a^{(2)} \right) \right\}, \quad (19)$$

where  $g_{\pi\rho\omega}$  is the  $\pi\rho\omega$  coupling [23] and the other coefficients have the same meaning as in the previous equation. At momenta much smaller than the meson masses, these short-range contributions are indeed contact interactions.

## IV. CROSS-SECTION

### A. The $pp \rightarrow d\pi^+$ reaction

We are concerned with evaluating the matrix elements of the above operators between the initial  ${}^3P_1$  and the deuteron final wave functions. To evaluate the influence of the potential in the amplitudes, we use Reid93 [44] and Argonne V18 [45] potentials which, for a given  $pp$  channel, are local potentials. Thus we evaluate the operators between coordinate space initial ( $i$ ) and final ( $f$ ) wave functions expressed by

$$\langle \vec{r} | i \rangle = \mp \frac{\sqrt{2}}{pr} i u_{1,1}(r) e^{i\delta_{1,1}} \left( \sqrt{2\pi} \sqrt{3} \right) |{}^3P_1\rangle, \quad (20)$$

where  $- (+)$  is for third-component of the angular momentum  $M_J = +1 (-1)$ , and

$$\langle \vec{r} | f \rangle = \frac{1}{r} \left[ u(r) |{}^3S_1\rangle + w(r) |{}^3D_1\rangle \right], \quad (21)$$

where the deuteron wave functions are normalized as

$$\int_0^\infty dr \left[ u^2(r) + w^2(r) \right] = 1. \quad (22)$$

Here and in the following the spin angular part is expressed, as usual, as

$$|{}^{2S+1}L_J\rangle = \sum_{m_L m_S} \langle L m_L S m_S | J m_J \rangle Y_L^{m_L}(\hat{\mathbf{r}}) \chi_S^{m_S}, \quad (23)$$

where  $Y_L$  is the spherical harmonic function.

We convert the operators of Eqs. (13-19) to configuration space by inverting the Fourier transforms. The resulting operators can then be used in configuration-space matrix elements. We define the matrix elements of the operators of Eqs. (13-19) as

$$\begin{aligned} \mathcal{M}^X &= \langle f | T^X | i \rangle \\ &= \mp \frac{\sqrt{12\pi} i}{p} e^{i\delta_{1,1}} \int_0^\infty dr \left[ \frac{u(r)}{\sqrt{m_\pi}} H_S^X(r) + \frac{w(r)}{\sqrt{2m_\pi}} H_D^X(r) \right] u_{1,1}(r), \end{aligned} \quad (24)$$

where  $X$  represents  $WT$ ,  $IA$ , *etc.*  $H_{S,D}^X(r)$  is the corresponding operator, obtained using the matrix elements given in the Appendix. To compare results before the cross-section evaluation, we define dimensionless amplitudes  $J^X$ , where  $X = WT, IA, \Delta$ , *etc.* via

$$\mathcal{M}^X = \mp \sqrt{12\pi} i e^{i\delta_{1,1}} \frac{g_A}{f_\pi^3} \cdot \frac{m_\pi}{4\pi} \sqrt{\frac{2}{3}} J^X. \quad (25)$$

We will plot  $J^X$  in terms of  $\eta$  to evaluate the energy dependence of the amplitude, and  $dJ^X/dr$  in terms of  $r$  to study the  $r$  dependence of the integrand.

The contribution from the Weinberg-Tomozawa term is given by

$$H_S^{WT}(r) = H_D^{WT}(r) = \frac{g_A}{4f_\pi^3} \frac{3m_\pi}{4\pi} \sqrt{\frac{2}{3}} \frac{(1 + \tilde{m}_\pi r)}{r^2} e^{-\tilde{m}_\pi r}, \quad (26)$$

where  $\tilde{m}_\pi = \sqrt{\frac{3}{4}}m_\pi$ . The Galilean correction to the WT term is given by

$$H_S^{GC}(r) = \frac{g_A}{4f_\pi^3} \frac{3m_\pi}{4\pi} \sqrt{\frac{2}{3}} \frac{m_\pi}{4m_N} [A_{GC}(r) + B_{GC}(r) + C_{GC}(r)], \quad (27)$$

$$H_D^{GC}(r) = \frac{g_A}{4f_\pi^3} \frac{3m_\pi}{4\pi} \sqrt{\frac{2}{3}} \frac{m_\pi}{4m_N} [A_{GC}(r) + B_{GC}(r) + D_{GC}(r)], \quad (28)$$

where

$$A_{GC}(r) = \frac{(1 + \tilde{m}_\pi r)}{r^2} e^{-\tilde{m}_\pi r}, \quad (29)$$

$$B_{GC}(r) = -2 \frac{e^{-\tilde{m}_\pi r}}{r} \left( 1 + \frac{2}{\tilde{m}_\pi r} + \frac{2}{(\tilde{m}_\pi r)^2} \right) \frac{\partial}{\partial r}, \quad (30)$$

$$C_{GC}(r) = 2 \frac{e^{-\tilde{m}_\pi r}}{r^2} \left( 1 + \frac{4}{\tilde{m}_\pi r} + \frac{4}{(\tilde{m}_\pi r)^2} \right), \quad (31)$$

$$D_{GC}(r) = 2 \frac{e^{-\tilde{m}_\pi r}}{r^2} \left( 1 + \frac{1}{\tilde{m}_\pi r} + \frac{1}{(\tilde{m}_\pi r)^2} \right). \quad (32)$$

The impulse approximation is given by

$$H_S^{IA}(r) = \frac{g_A}{f_\pi} \frac{m_\pi}{m_N} \sqrt{\frac{1}{3}} \left[ \frac{1}{r} + \frac{\partial}{\partial r} \right], \quad (33)$$

$$H_D^{IA}(r) = \frac{g_A}{f_\pi} \frac{m_\pi}{m_N} \sqrt{\frac{1}{3}} \left[ -\frac{2}{r} + \frac{\partial}{\partial r} \right]. \quad (34)$$

The  $\Delta$  resonance contribution be written as

$$H_S^\Delta(r) = \frac{1}{9m_N} \left( \frac{g_A}{f_\pi} \right)^3 \left( \frac{h_A}{g_A} \right)^2 \frac{m_\pi \tilde{m}_\pi^2}{(m_\pi - \delta)} \sqrt{\frac{2}{3}} \frac{1}{4\pi} [A_\Delta(r) + B_\Delta(r) + C_\Delta(r)], \quad (35)$$

$$H_D^\Delta(r) = \frac{1}{9m_N} \left( \frac{g_A}{f_\pi} \right)^3 \left( \frac{h_A}{g_A} \right)^2 \frac{m_\pi \tilde{m}_\pi^2}{(m_\pi - \delta)} \sqrt{\frac{2}{3}} \frac{1}{4\pi} [A_\Delta(r) + B_\Delta(r) + D_\Delta(r)], \quad (36)$$

where

$$A_\Delta(r) = 2 \frac{(1 + \tilde{m}_\pi r)}{r^2} e^{-\tilde{m}_\pi r}, \quad (37)$$

$$B_\Delta(r) = -2 \frac{e^{-\tilde{m}_\pi r}}{r} \left( 1 + \frac{1}{\tilde{m}_\pi r} + \frac{1}{(\tilde{m}_\pi r)^2} \right) \frac{\partial}{\partial r}, \quad (38)$$

$$C_\Delta(r) = 2 \frac{e^{-\tilde{m}_\pi r}}{r^2} \left( 1 + \frac{2}{\tilde{m}_\pi r} + \frac{2}{(\tilde{m}_\pi r)^2} \right), \quad (39)$$

$$D_\Delta(r) = \frac{e^{-\tilde{m}_\pi r}}{r^2} \left( -1 + \frac{1}{\tilde{m}_\pi r} + \frac{1}{(\tilde{m}_\pi r)^2} \right). \quad (40)$$

The isospin-independent seagull term is given by

$$H_S^{SG}(r) = H_D^{SG}(r) = \frac{g_A m_\pi^2}{f_\pi^3 4\pi} \sqrt{\frac{2}{3}} F_{SG} \frac{(1 + \tilde{m}_\pi r)}{r^2} e^{-\tilde{m}_\pi r}, \quad (41)$$

where

$$F_{SG} = 4c_1 + \frac{\delta m_N}{4m_\pi^2} - \left( c_2 + c_3 - \frac{g_A^2}{8m_N} \right). \quad (42)$$

We also include the effects of the  $\sigma$  and  $\omega$  exchange and  $\rho - \omega$  term. The result for the  $\sigma$  and  $\omega$  exchange is

$$H_S^{\sigma,\omega}(r) = \frac{g_A m_\pi}{f_\pi m_N^2} \sqrt{\frac{2}{3}} \left\{ [f_\sigma(r) + f_\omega(r)] \left( \frac{\partial}{\partial r} + \frac{1}{r} \right) + \frac{1}{2} \frac{\partial}{\partial r} [f_\sigma(r) + f_\omega(r)] \right\}, \quad (43)$$

and

$$H_D^{\sigma,\omega}(r) = \frac{g_A m_\pi}{f_\pi m_N^2} \sqrt{\frac{2}{3}} \left\{ [f_\sigma(r) + f_\omega(r)] \left( \frac{\partial}{\partial r} - \frac{2}{r} \right) + \frac{1}{2} \frac{\partial}{\partial r} [f_\sigma(r) + f_\omega(r)] \right\}, \quad (44)$$

where the function  $f_h(r)$  accounts for exchange of the meson  $h$  between nucleons,

$$f_h(r) = \frac{g_h^2 e^{-m_h r}}{4\pi r}. \quad (45)$$

We follow Ref. [7] by including the effects of form factors in these heavy-meson contributions, as given in the Bonn potential [46]. For completeness, we repeat that monopole form factors are used at each meson vertex according to the replacement

$$g_h \rightarrow g_h \frac{\Lambda_h^2 - m_h^2}{\Lambda_h^2 - k_\mu k^\mu}, \quad (46)$$

where  $k_\mu$  is the transferred momentum and  $\Lambda_h$  is the cutoff mass.

With  $M$  denoting the common  $\rho - \omega$  mass (780 MeV),  $\rho - \omega$  exchange yields

$$H_S^{\rho-\omega}(r) = \frac{g_\rho g_\omega g_{\pi\rho\omega} m_\pi}{4m_N^2 4\pi} \sqrt{\frac{2}{3}} \frac{2(2 + C_\rho)}{M(\Lambda^2 - M^2)} \times \left\{ [A_{\rho-\omega}(r; M, \Lambda) - A_{\rho-\omega}(r; \Lambda, M)] \left( \frac{\partial}{\partial r} + \frac{1}{r} \right) - [B_{\rho-\omega}(r; M, \Lambda) - B_{\rho-\omega}(r; \Lambda, M)] \left( \frac{\partial}{\partial r} - \frac{1}{r} \right) \right\}, \quad (47)$$

where

$$A_{\rho-\omega}(r; m_1, m_2) = m_1 \frac{e^{-m_1 r}}{m_1 r} \left[ 4m_1^2 \left( \frac{1}{m_1 r} + \frac{1}{(m_1 r)^2} \right) - (m_2^2 - m_1^2) m_1 r + 3m_1^2 + m_2^2 \right],$$

$$B_{\rho-\omega}(r; m_1, m_2) = m_1 \frac{e^{-m_1 r}}{m_1 r} \left[ 4m_1^2 \left( 1 + \frac{3}{m_1 r} + \frac{3}{(m_1 r)^2} \right) - (m_2^2 - m_1^2)(1 + m_1 r) \right]. \quad (48)$$

$H_D^{\rho-\omega}(r)$  can be obtained making the replacement

$$\left(\frac{\partial}{\partial r} \pm \frac{1}{r}\right) \longrightarrow \left(\frac{\partial}{\partial r} \pm \frac{2}{r}\right)$$

above.

The final steps consist of computing the total matrix element  $\mathcal{M}$ ,

$$\mathcal{M} = \mathcal{M}^{WT} + \mathcal{M}^{GC} + \mathcal{M}^{IA} + \mathcal{M}^{ST} + \mathcal{M}^\Delta + \mathcal{M}^{\sigma,\omega} + \mathcal{M}^{\rho-\omega}, \quad (49)$$

squaring it, and integrating over the available phase space. We find

$$\sigma = \frac{1}{16\pi} \frac{m_\pi}{p} E_d \omega_q \eta |\mathcal{M}|^2, \quad (50)$$

where  $p$  is the magnitude of the center-of-mass 3-momentum,

$$p = m_\pi \cdot \sqrt{\frac{m_N}{m_\pi} \cdot \sqrt{1 + \eta^2} + \frac{\eta^2 m_N}{2M_d} + \frac{(M_d - 2m_N)m_N}{m_\pi^2}},$$

and  $E_d$  is energy of the produced deuteron of mass  $M_d$ ,  $E_d = \sqrt{M_d^2 + q^2}$ .

## B. The $pp \rightarrow pn\pi^+$ reaction

As we did in the deuteron case, we evaluate the matrix elements for the unbound final state using the same operators of Eqs. (13)-(19). We will consider here just the absolute threshold limit where  $L_{\pi(NN)} = 0$ . According to selection rules, we have 2 channels, as stated in Tab. I:  ${}^3P_1 \rightarrow {}^3S_1$  ( $T_i = 1, T_f = 0$ ) and  ${}^3P_0 \rightarrow {}^1S_0$  ( $T_i = 1, T_f = 1$ ). Again, to evaluate the influence of the potential in the amplitudes, we use Reid93 [44] and Argonne V18 [45] potentials which, for a given  $pp$  or  $pn$  channel, are local potentials. Thus we evaluate the operators between coordinate space initial ( $i$ ) and final ( $f$ ) wave functions for the two channels, expressed by

- ${}^3P_1 \rightarrow {}^3S_1$  channel:

$$\begin{aligned} \langle \vec{r} | i \rangle &= \mp \frac{\sqrt{2}}{pr} i u_{1,1}(r) e^{i\delta_{1,1}} \left( \sqrt{2\pi} \sqrt{3} \right) |{}^3P_1\rangle, \\ \langle \vec{r} | f \rangle &= \frac{1}{p'r} i u_{0,1}(r) e^{i\delta_{0,1}} \sqrt{4\pi} |{}^3S_1\rangle, \end{aligned} \quad (51)$$

- ${}^3P_0 \rightarrow {}^1S_0$  channel:

$$\begin{aligned} \langle \vec{r} | i \rangle &= \frac{\sqrt{2}}{pr} i u_{1,0}(r) e^{i\delta_{1,0}} \sqrt{4\pi} |{}^3P_0\rangle, \\ \langle \vec{r} | f \rangle &= \frac{1}{p'r} i u_{0,0}(r) e^{i\delta_{0,0}} \sqrt{4\pi} |{}^1S_0\rangle, \end{aligned} \quad (52)$$

where  $- (+)$  is for third-component of the angular momentum  $M_J = +1 (-1)$ .

We convert the operators of Eqs. (13-19) to configuration space by inverting the Fourier transforms. The resulting operators can then be used in configuration-space matrix elements. We define the matrix elements of the operators of Eqs. (13-19) as

- ${}^3P_1 \rightarrow {}^3S_1$  channel

$$\mathcal{M}^X = \langle {}^3S_1 | T^X | {}^3P_1 \rangle = \mp 4\pi \sqrt{3} i e^{i(\delta_{0,1} + \delta_{1,1})} \frac{g_A}{f_\pi^3} \cdot \frac{1}{4\pi} \sqrt{\frac{2}{3}} J^X. \quad (53)$$

- ${}^3P_0 \rightarrow {}^1S_0$  channel

$$\mathcal{M}^Y = \langle {}^1S_0 | T^Y | {}^3P_0 \rangle = 4\pi \sqrt{2} i e^{i(\delta_{1,0} + \delta_{0,0})} \frac{g_A}{f_\pi^3} \cdot \frac{1}{4\pi} J^Y. \quad (54)$$

with

$$J^X = \frac{m_\pi}{p p'} \int_0^\infty dr u_{0,1} H^X(r) u_{1,1}(r) \quad (55)$$

$$J^Y = \frac{m_\pi}{p p'} \int_0^\infty dr u_{0,0} H^Y(r) u_{1,0}(r) \quad (56)$$

where  $X$  and  $Y$  represents  $\Delta$ ,  $IA$ , etc.,  $J^X$  and  $J^Y$  are dimensionless integrals,  $H^X(r)$  and  $H^Y(r)$  are the corresponding operators, obtained using the matrix elements given in the Appendix, which are the same used in the deuteron final state (for the  ${}^3P_1 \rightarrow {}^3S_1$  channel) and in the  $pp \rightarrow pp\pi^0$  [22] (for the  ${}^3P_0 \rightarrow {}^1S_0$  channel). We will plot  $J^X$  and  $J^Y$  in terms of  $p'$  to evaluate the energy dependence of the amplitude, and  $dJ^X/dr$  and  $dJ^Y/dr$  in terms of  $r$  to study the  $r$  dependence of the integrand.

For the  ${}^3P_1 \rightarrow {}^3S_1$  channel, the coordinate space expressions for the amplitudes are pretty much the same of the  $S$ -wave deuteron amplitudes. For instance, the Weinberg-Tomozawa term gives

$$H^{WT}(r) = \frac{3}{4} \frac{(1 + \tilde{m}_\pi r)}{r^2} e^{-\tilde{m}_\pi r}, \quad (57)$$

where  $\tilde{m}_\pi = \sqrt{\frac{3}{4}} m_\pi$ . For the  ${}^3P_0 \rightarrow {}^1S_0$  channel, the expressions follow closely the work of Cohen *et al* [22], the isospin matrix elements being the only difference. As we did in the deuteron case, we include the effects of form factors when dealing with heavy meson contributions.

The final steps consist of computing the total matrix element  $\mathcal{M}$  for the two channels, using Eq. (49) for the  ${}^3S_1$  final state and the same equation but without WT and the GC terms for the  ${}^1S_0$  final state, since in this state the isovector contributions are zero.

The cross section is obtained by squaring the total amplitude, and integrating over the available phase space. We find



$$\sigma = \sum_{spins} \frac{1}{v} \int_0^{p'_{max}} dp' \frac{p'^2 q}{(2\pi)^3} |\mathcal{M}|^2 \frac{m_n}{2m_n + w(q)} \quad (58)$$

where  $v$  is the laboratory velocity of the incident proton,  $q$  is the pion 3-momentum,  $w(q) = \sqrt{q^2 + m_\pi^2}$ ,  $p$  is the magnitude of the center-of-mass initial 3-momentum and  $p'_{max} = \sqrt{p^2 - m_N m_\pi}$ . The  $\Sigma_{spins}$  indicates that (a) a sum over final spin states and (b) an average over initial spin states must be made, which result in factors of 3/4 for the  ${}^3S_1$  and 1/4 for the  ${}^1S_0$  final states.

## V. INPUT PARAMETERS AND RESULTS

The various amplitudes considered in the last section depend on several parameters that we can determine from other processes. The WT, GC to WT, and the impulse-approximation operators depend on the pion mass,  $m_\pi = 138$  MeV [47], and on

$$\frac{g_A}{f_\pi} = \frac{g_{\pi NN}}{m_N}; \quad (59)$$

we use the value of  $g_{\pi NN}$  appropriate for each potential. The  $\Delta$  operator of Eq.(16) further depends on the  $\Delta - N$  mass splitting  $\delta = 294$  MeV [47] and on the  $\pi N \Delta$  coupling constant,  $h_A$ . This has been fixed from  $P$ -wave  $\pi N$  scattering (see, e.g., Ref. [48]),

$$\frac{h_A}{g_A} \simeq 2.1. \quad (60)$$

The seagull operator of Eq.(17) depends on four parameters  $c_{1,2,3}$  and  $\delta m_N$ . The  $c_i$ 's can be obtained by fitting  $S$ -wave  $\pi N$  scattering. In Ref. [13] they were found to be

$$\left[ 4c_1 + \frac{\delta m_N}{4m_\pi^2} - \left( c_2 + c_3 - \frac{g_A^2}{8m_N} \right) \right] = -\frac{2.31}{2m_N}, \quad (61)$$

from the  $\sigma$ -term, the isospin-even scattering length, and the axial polarizability, to  $\mathcal{O}(Q^3)$ . We refer to this as ‘‘Seal’’. A different determination from an  $\mathcal{O}(Q^2)$  fit to  $\pi N$  sub-threshold parameters [31] gives  $-0.29/2m_N$  instead. We refer to this as ‘‘SealI’’. Newer determinations [30] give values closer to the more negative value, but we use both values in order to estimate the importance of this contribution. Note that the analysis of Ref. [13] does not include the isobar explicitly. Since the inclusion of the  $\pi N \Delta$  interaction only affects  $S$  waves at one order higher than the  $c_i$ 's, the above values can still be used to estimate the effect of  $S$ -wave rescattering. The parameter,  $\delta m_N$ , can in principle also be determined from  $S$ -wave  $\pi N$  scattering, but would require a careful analysis of other isospin-violating effects. Chiral symmetry relates it to the strong interaction contribution to the nucleon mass splitting, which is also difficult to determine directly. Estimates of the electromagnetic contribution  $\bar{\delta} m_N$  are more reliable,  $\bar{\delta} m_N \sim -1.5$  MeV [49], and give  $\delta m_N \sim 3$  MeV. To be definite, we use

$$\delta m_N = 3 \text{ MeV}. \quad (62)$$

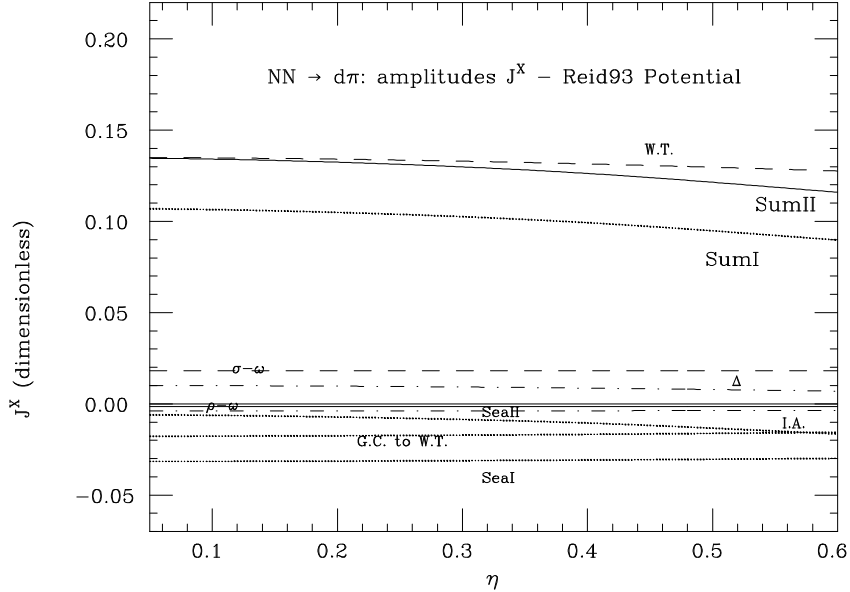


FIG. 2. Matrix elements  $J$  as function of  $\eta$  for the various contributions to  $pp \rightarrow d\pi^+$ , calculated with wavefunctions from the Reid93 potential.

Finally, the  $\sigma, \omega$  and the  $\rho - \omega$  operators involve  $g_h, \Lambda_h, m_h,$  and  $C_\omega$ , parameters listed in Table A.3 of Ref. [46]. They also involve  $g_{\pi\rho\omega}$ , discussed in Ref. [23]. These heavy-meson contributions correspond to chiral Lagrangian coefficients of natural size:  $d'_1 + e_1 \approx -1.5(1/f_\pi^2 M)$ ,  $e_1 \approx -2(1/f_\pi^2 M)$ ,  $e_2 \approx 2(1/f_\pi^2 M)$ , and  $g \approx 4(1/f_\pi^2 M^3)$ .

### A. The $pp \rightarrow d\pi^+$ reaction

The relative sizes of the various contributions to the matrix element  $J$  of this reaction as function of  $\eta$  are shown in Fig. 2 for the Reid93 potential and in Fig. 3 for the AV18 potential. There is a very strong similarity between these two sets of results.

Our leading order comprises WT, IA and  $\Delta$ . The first noticeable observation is that WT is by far the largest contribution. This is a consequence of cancellations in IA and  $\Delta$  which were not anticipated by the power counting. In Figs. 4, 5, and 6 we can see typical integrands for the three contributions at  $\eta = 0.3$ , in the case of the Argonne V18 potential. While for WT the contributions from the  $S$  and  $D$  deuteron waves add and are dominated by the region around  $r = 1.5$  fm, for IA and  $\Delta$  the  $S$  and  $D$  waves tend to interfere destructively, and contributions from different  $r$  regions approximately cancel.

Our formally sub-leading contributions are all considerably smaller than WT. This suggests that the theoretical control of this reaction is greater than for  $pp \rightarrow pp\pi^0$ . Moreover, sub-leading contributions come with different signs, partially cancelling. In fact, the  $\sigma, \omega$  and GC terms come out with similar size —as predicted by the power counting— but with opposite signs; there is an almost complete accidental cancellation between them.  $\rho - \omega$  exchange is of higher order and indeed very small. As a result, when the small contribution from the combination of seagull parameters “SeaII” is considered, the sum of all sub-leading

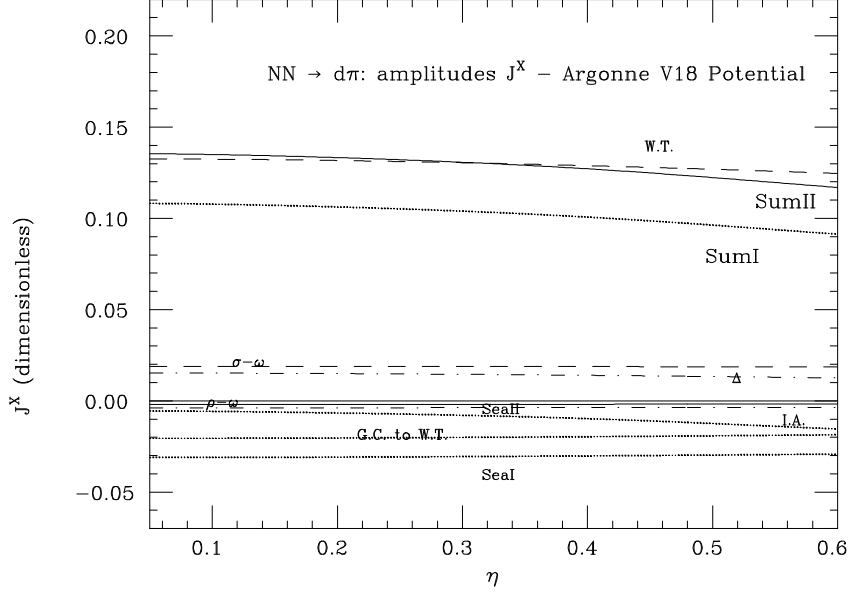


FIG. 3. Matrix elements  $J$  as function of  $\eta$  for the various contributions to  $pp \rightarrow d\pi^+$ , calculated with wavefunctions from the Argonne V18 potential.

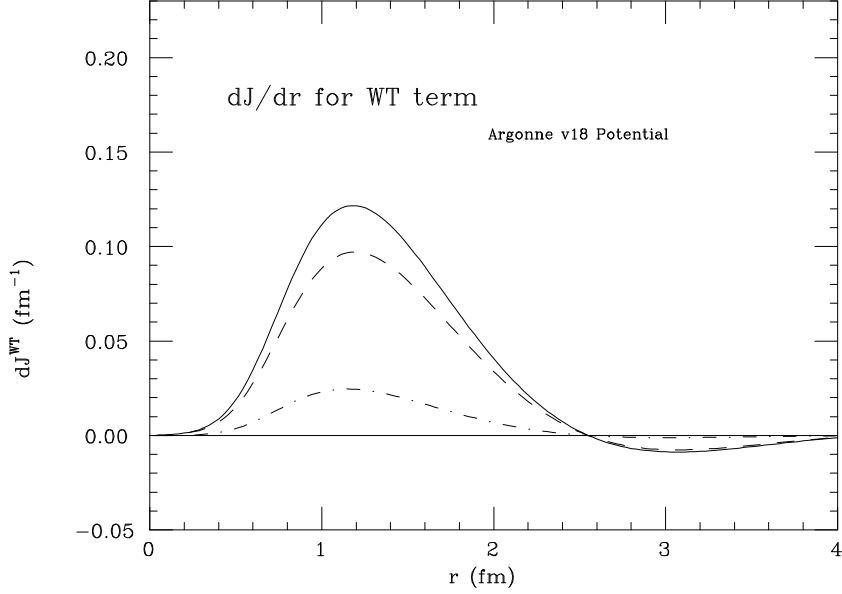


FIG. 4. Typical integrands ( $\eta = 0.3$ ) of the Weinberg-Tomozawa contribution to  $pp \rightarrow d\pi^+$  as function of the radial coordinate  $r$  for deuteron  $S$  and  $D$  waves of the Argonne V18 potential. The  $S$  wave is given by the dashed line, the  $D$  wave by the dot-dashed line and the sum by the solid line.

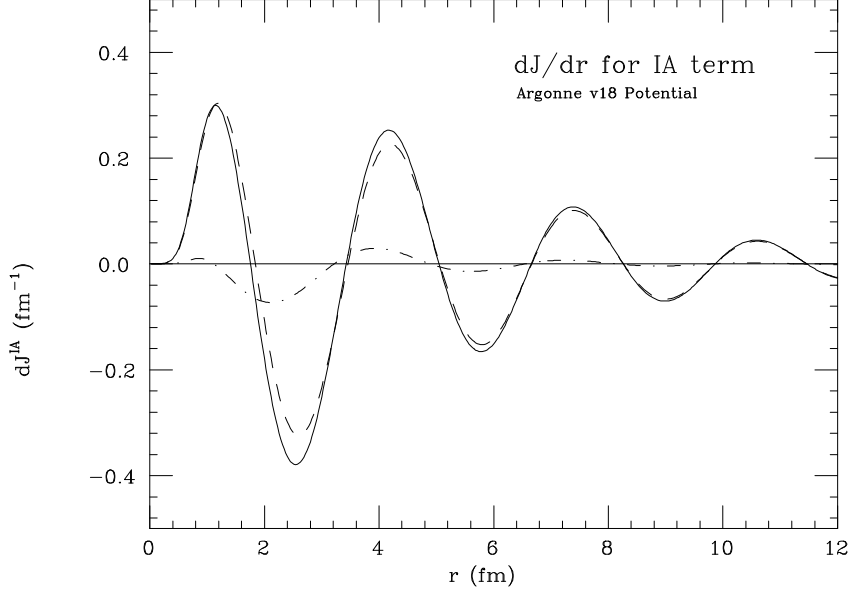


FIG. 5. Typical integrands ( $\eta = 0.3$ ) of the impulse contribution to  $pp \rightarrow d\pi^+$  as function of the radial coordinate  $r$  for deuteron  $S$  and  $D$  waves of the Argonne V18 potential. Lines are as in Fig. 4.

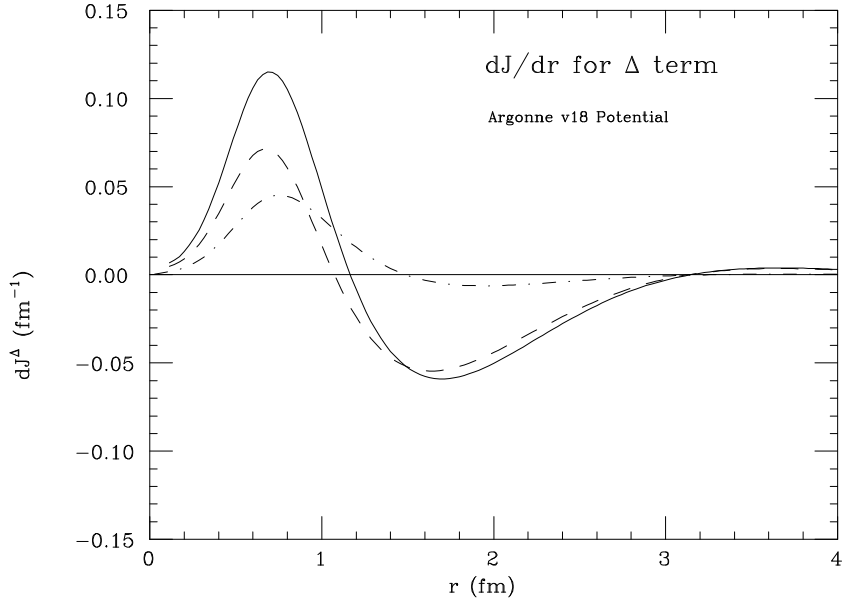


FIG. 6. Typical integrands ( $\eta = 0.3$ ) of the delta contribution to  $pp \rightarrow d\pi^+$  as function of the radial coordinate  $r$  for deuteron  $S$  and  $D$  waves of the Argonne V18 potential. Lines are as in Fig. 4.

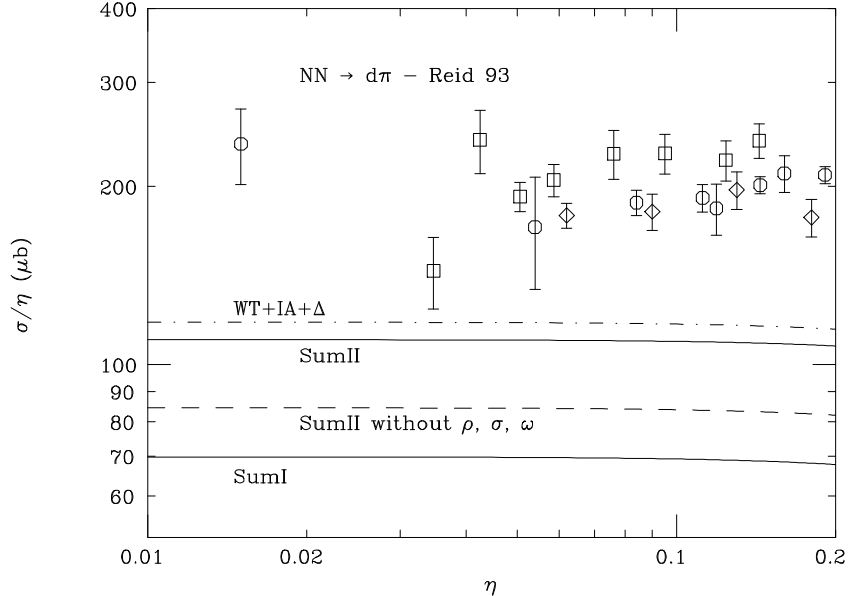


FIG. 7. Reduced cross-section  $\sigma/\eta$  for  $pp \rightarrow d\pi^+$  as function of  $\eta$  calculated with the Reid93 potential in leading order ( $WT + IA + \Delta$ ), in leading plus sub-leading order with two sets of parameters (SumI and SumII), and in leading plus sub-leading order without heavy-meson exchange (SumII without  $\rho, \sigma, \omega$ ), and compared with data from TRIUMF (circles) [37], COSY (diamonds) [38] and IUCF (squares) [39].

contributions is small. The sum is somewhat larger and of opposite sign to leading order when “SeaI” is used.

In Fig. 7 we compare our leading and sub-leading results for the  $pp$  cross-section (without Coulomb) using the Reid93 potential with data from Refs. [37–39]. We see that our curves are approximately constant, as expected. Recent data points for  $\eta < 0.1$  are not all consistent, but they cluster around an average  $\alpha$  of about 180 to 190  $\mu\text{b}$ . The value of  $\alpha$  in leading order ( $WT+IA+\Delta$ ) is a factor of about 1.5 below data. The destructive interference with next-order contributions increases the disagreement by an amount depending on the value of  $\pi N$  isoscalar rescattering term. The change is bigger when “SeaI” is used. This can be seen in Fig. 7 as “SumI” and “SumII”. Because of the cancellations among sub-leading terms, the result exhibits comparable dependence on the short-range contributions, as can be seen in Fig. 7 as “SumII without  $\sigma, \rho, \omega$ ”. We summarize our results in Fig. 8 where we show the sum of all the contributions we considered for the two sets of seagull parameters, and for the two potentials.

## B. The $pp \rightarrow pn\pi^+$ reaction

The relative sizes of the various contributions to the matrix element  $J$  of this reaction as function of  $p'$  are shown for the  $^3S_1$  final state in Fig. 9 for the Reid93 potential and in Fig. 10 for the AV18 potential; and for the  $^1S_0$  final state in Fig. 11 for the Reid93 potential and in Fig. 12 for the AV18 potential.

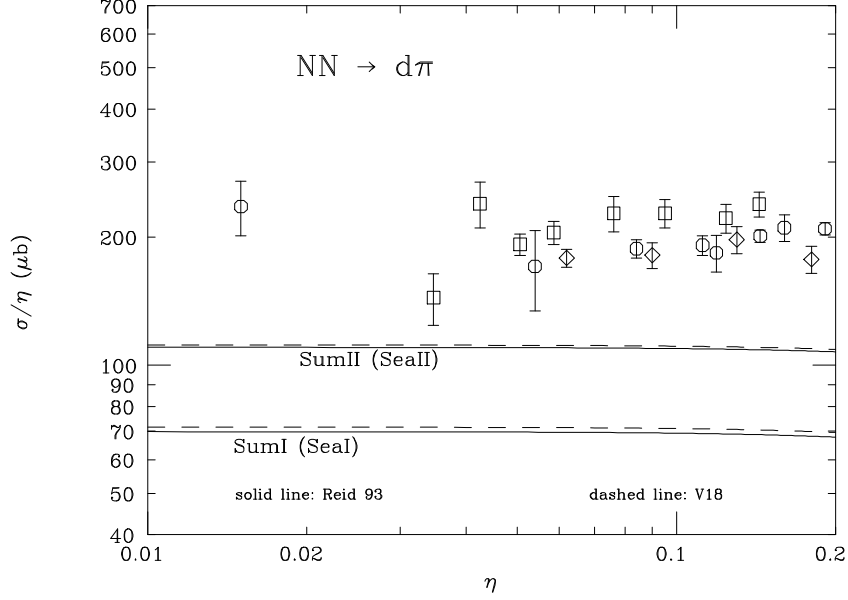


FIG. 8. Reduced cross-section  $\sigma/\eta$  for  $pp \rightarrow d\pi^+$  as function of  $\eta$  for the sum of all the contributions considered with two sets parameters (SumI, SumII) for the Reid93 (solid line) and Argonne V18 (dashed line) potentials, compared with data from TRIUMF (circles) [37], COSY (diamonds) [38] and IUCF (squares) [39].

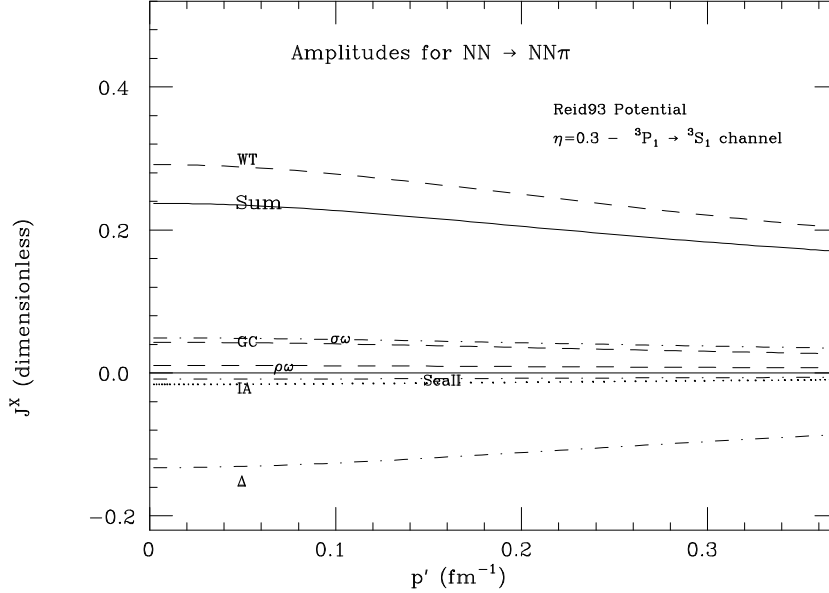


FIG. 9. Matrix elements  $J$  as function of  $p'$  for the various contributions to  $pp \rightarrow pn\pi^+$ , calculated with wavefunctions from the Reid93 potential:  ${}^3S_1$  final state.

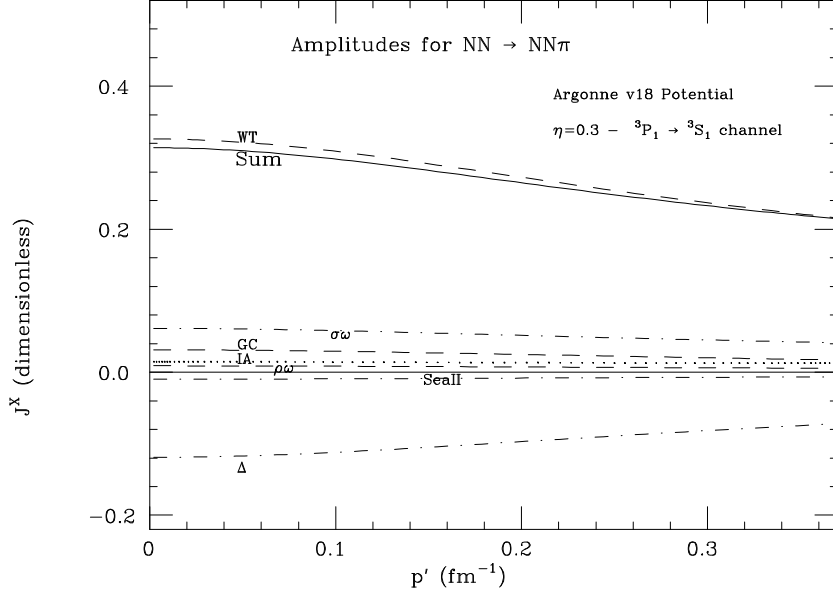


FIG. 10. Matrix elements  $J$  as function of  $p'$  for the various contributions to  $pp \rightarrow pn\pi^+$ , calculated with wavefunctions from the Argonne V18 potential:  ${}^3S_1$  final state.

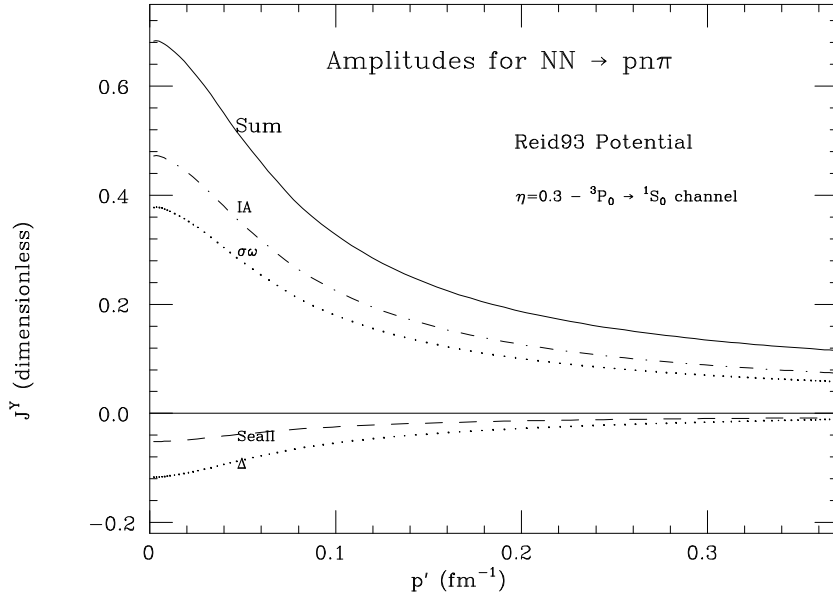


FIG. 11. Matrix elements  $J$  as function of  $p'$  for the various contributions to  $pp \rightarrow pn\pi^+$ , calculated with wavefunctions from the Reid93 potential:  ${}^1S_0$  final state.

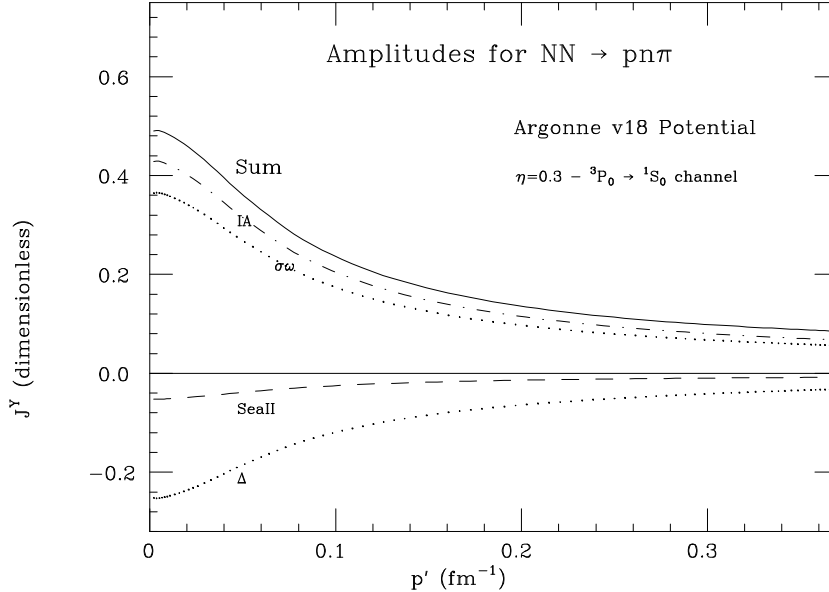


FIG. 12. Matrix elements  $J$  as function of  $p'$  for the various contributions to  $pp \rightarrow pn\pi^+$ , calculated with wavefunctions from the Argonne V18 potential:  $^1S_0$  final state.

Here again the WT contribution is the largest; since it contributes only to the  $^3S_1$  final state, this channel is dominant. Most of the other contributions are much smaller and tend to cancel to some extent. The exception is the  $\Delta$ , which has a significant destructive interference with WT in the  $^3S_1$  state. The IA contribution is small due to the same type of cancellation observed before among different regions in coordinate space.

In Fig. 13 we compare our results for the different final states using the Reid93 potential with data from Ref. [40,41]. In Fig. 14 we summarize our results for the two potentials considered and compare them to the same data. We see that the theory produces a correct shape for the  $\eta$  dependence but fails in magnitude by a factor of  $\sim 5$ . Use of “SeaI” further worsens the results. Once again the differences between the two potentials are minimal.

### C. Discussion

The  $d\pi^+$  final state has been considered before in the literature. Ref. [2] has found that the impulse term was very small due to the strong cancellation between the  $S$  and  $D$  waves in the matrix element shown above. Mostly due to the WT,  $\alpha$  of 146 to 160  $\mu\text{b}$  was obtained using the older, higher value of the  $\pi NN$  coupling constant; using the more recent value, we get 124 to 136  $\mu\text{b}$ . A similar analysis [50] included also form factors at the  $\pi\pi NN$  vertices, which led to a decrease of approximately 20% in the cross section; with the more modern coupling constants, the overall result was near 100  $\mu\text{b}$ . Recently, Ref. [33] re-analyzed this reaction using a covariant approach. The result for  $\alpha$  using only the WT term was again near 100  $\mu\text{b}$ , but the amplitude contains what we refer to as the Galilean correction to the WT term, which has an opposite sign. Our results for the WT term alone are in numerical agreement with these works, since we find that it gives an  $\alpha$  of about 100  $\mu\text{b}$ .



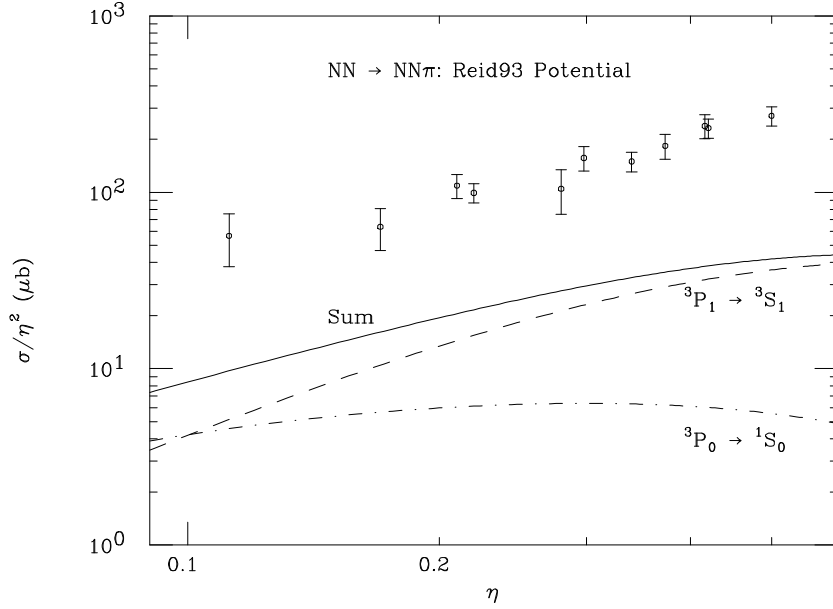


FIG. 13. Reduced cross-section  $\sigma/\eta^2$  for  $pp \rightarrow pn\pi^+$  as function of  $\eta$  calculated with the Reid93 potential:  $^3S_1$  final state (dashed line),  $^1S_0$  final state (dash-dotted line), their sum (solid line), and data from IUCF [40,41].

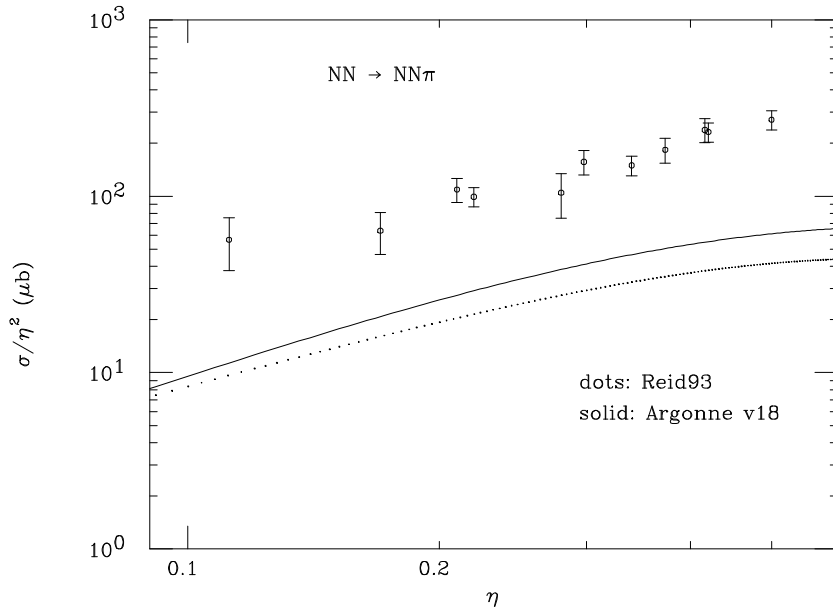


FIG. 14. Reduced cross-section  $\sigma/\eta^2$  for  $pp \rightarrow pn\pi^+$  as function of  $\eta$  for the sum of all the contributions: Reid93 potential (dotted line), Argonne V18 potential (solid line), and data from IUCF [40,41].

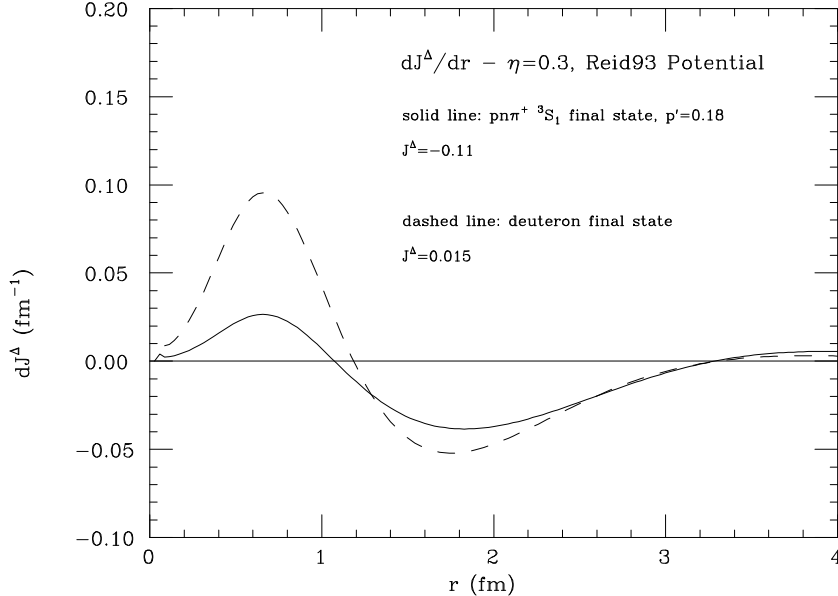


FIG. 15. Typical integrands ( $\eta = 0.3$ ) of the delta contribution as function of the radial coordinate  $r$  for the  ${}^3S_1$   $pn$  final state at  $p' = 0.18$  (solid line) compared to the deuteron final state (dashed line).

Other contributions tend to worsen the description of the data. Particularly damaging are the contributions of the rescattering type. Here, as for  $pp \rightarrow pp\pi^0$ , the  $S$ -wave seagulls tend to interfere destructively with the leading mechanism.

As in the case of the  $pp \rightarrow pp\pi^0$  reaction, the  $\Delta$  contribution shows appreciable dependence on the potential used. But unlike that reaction, here it generates relatively small dependence on the potential in the final result, as consequence of the large relative size of WT. The  $\Delta$  contribution is the one that presents the largest change when we compare  $pn$  and  $d$  final states. In Fig. 15 we compare the radial distributions of the delta contribution for the  ${}^3S_1$   $pn$  final state at  $p' = 0.18 \text{ fm}^{-1}$  and for the deuteron final state (same as in Fig. 6). From this we can see how this contribution has different signs in the two channels, being small and constructive with WT for  $d$  ( $J_d^{WT} = 0.130$  and  $J_d^\Delta = 0.015$ ;  $\eta = 0.3$ ) and larger and destructive for  $pn$  ( $J_{pn}^{WT} = 0.260$  and  $J_{pn}^\Delta = -0.11$ ;  $\eta = 0.3$ ;  $p' = 0.18$ )

Note, however, that the  $\Delta$  contribution is subject to large uncertainties. First, the  $\pi N\Delta$  coupling constant is not well determined and appears squared; although we do not know whether this coupling should be bigger or smaller than the value used here, it could contribute to a decrease of the  $\Delta$  effect. Second, the  $\pi N\Delta$  form factor seems to be much softer than the corresponding  $\pi NN$  form factor; our neglecting both enhances the  $\Delta$  contribution relative to the WT term. Third, we have neglected the  $\Delta - N$  mass difference in energies; since the  $\Delta$  mass would appear in the denominator, the delta contribution would decrease by a factor of  $\sim 2m_N/(m_N + m_\Delta)$ . Fourth, we have neglected the kinetic energy of the delta, account of which would further decrease its amplitude. Fifth, it is known that there can be some cancellation between the pion- and rho-exchange delta terms; including the latter would also diminish the delta contribution. Assuming each of these gives a 10% decrease, we could very well be overestimating the  $\Delta$  contribution by 50% or more.

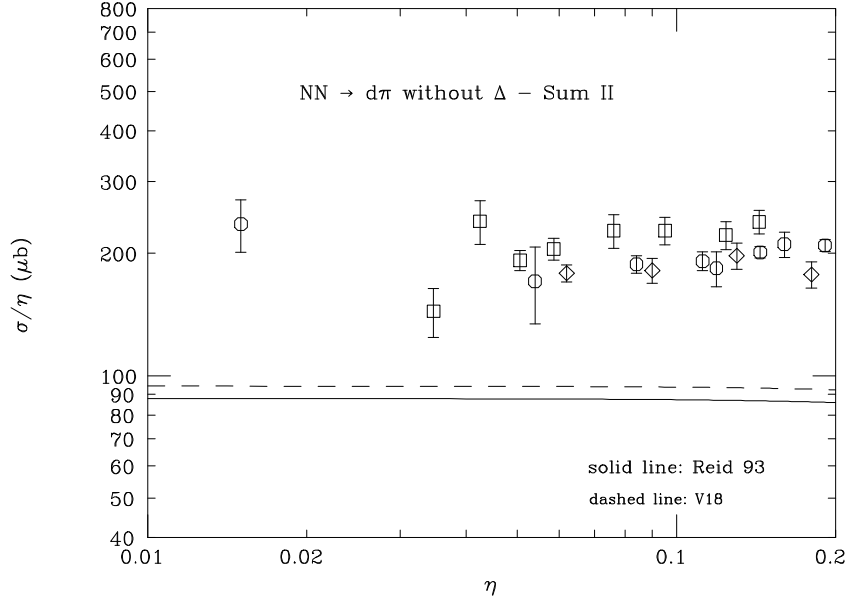


FIG. 16. Reduced cross-section  $\sigma/\eta$  for  $pp \rightarrow d\pi^+$  as function of  $\eta$ . The graph show the sum of all the contributions, excluding the  $\Delta$ : Reid93 potential (dotted line), Argonne V18 potential (solid line), and data from TRIUMF (circles) [37], COSY (diamonds) [38] and IUCF (squares) [39].

If we neglect this contribution altogether, we obtain the results in Fig. 16 for the cross section in the  $d$  channel and in Fig. 17 for the cross section in the  $pn$  channel. This brings theory to underestimate both sets of data by a common factor of  $\simeq 2$ . This implies that there must be further corrections to the amplitude of about 50%. This is not unlike the  $pp \rightarrow pp\pi^0$  reaction considered in Ref. [23], where theory tends to fail by a similar factor. The case for failure of theory there is less clear-cut, however, because of the lack of a large contribution as for the WT term here. As a consequence, the usually small effect of other mechanisms is enhanced and the result is dominated by shorter-range dynamics; more sensitivity to the potential and seagull terms surfaces, and it is possible to find a combination of parameters that includes data [23]. No such gimmicks work here. For example, we find that heavy-meson exchange —hailed as solution in the  $pp \rightarrow pp\pi^0$  reaction— does not help much in  $\rightarrow d\pi^+$  and  $\rightarrow pn\pi^+$ , in agreement with the findings in Refs. [42,43]. The dependence on the  $\Delta$  contribution (which is a particular type of rescattering) suggests that we need better control over longer-range contributions, such as  $\pi N$  rescattering and two-pion exchange.

## VI. CONCLUSION

We have calculated the cross section near threshold for the reactions  $pp \rightarrow d\pi^+, \rightarrow pn\pi^+$ , using a chiral power counting to order interactions. The interactions included contain most of the interactions found in the literature. In particular, they include mechanisms used in various models of the  $pp \rightarrow pp\pi^0$  reaction. In contrast to the latter, results here depend relatively little on the wavefunction employed and on short-range interactions. The Weinberg-Tomozawa term dominates, but the delta contribution can be important, with

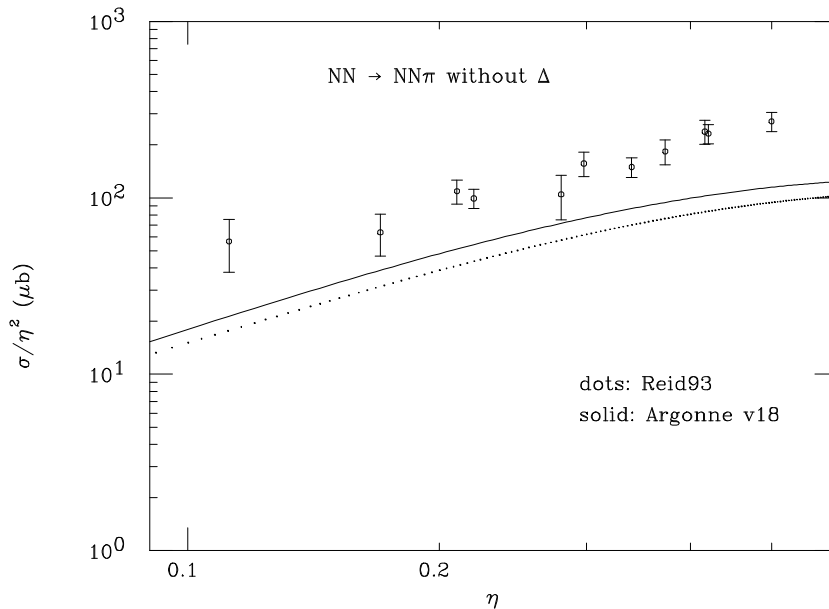


FIG. 17. Reduced cross-section  $\sigma/\eta^2$  for  $pp \rightarrow pn\pi^+$  as function of  $\eta$ . The lines shown the sum of all the contributions, excluding the  $\Delta$ : Reid93 potential (dotted line), Argonne V18 potential (solid line), and data from IUCF [40,41].

large uncertainty. Our computed results typically fall a factor of about two below the data. Our kernels vary as the cube of a generic meson-nucleon coupling constant, so such discrepancy can be parametrized as a 12% deficiency in the coupling constants. The pion-nucleon coupling constant is known to higher precision than that, but not to much higher precision. Thus the discrepancy we find might not be a very serious problem.

Our main conclusion is that a relatively long-range mechanism — such as  $\pi N$  rescattering and/or two-pion exchange — is needed for the description of these reactions. Accordingly, we suggest that advance in understanding pion production in  $NN$  collisions must follow not from the study of  $pp \rightarrow pp\pi^0$  by itself — as has been the trend of theoretical study to date — but from focus on an understanding of long-range effects that afflict all channels.

## Acknowledgments

We thank C. Hanhart for a helpful discussion. This research was supported in part by the U.S. DOE under grant DE-FG03-97Er41014 and NSF under grant PHY 94-20470. The work of C.A.dR. was supported by the Brazilian FAPESP under contract numbers 97/05817-0 and 97/6209-4. He thanks the Nuclear Theory group at the University of Washington for hospitality during the initial stages of this work.

## Appendix

The calculation of the cross-section in Section IV relies on the following matrix elements. For isospin,

$$\langle 00 | i\epsilon_{abc} \tau_b^{(1)} \tau_c^{(2)} | 11 \rangle = -2 , \quad (63)$$

$$\langle 00 | \vec{A} \tau_a^{(1)} - \vec{B} \tau_a^{(2)} | 11 \rangle = \vec{A} + \vec{B} , \quad (64)$$

$$\langle 00 | \vec{A} \tau_3^{(1)} \tau_a^{(2)} - \vec{B} \tau_a^{(1)} \tau_3^{(2)} | 11 \rangle = -(\vec{A} + \vec{B}) , \quad (65)$$

$$\langle 00 | \delta_{3a} \vec{\tau}^{(1)} \cdot \vec{\tau}^{(2)} | 11 \rangle = 0 , \quad (66)$$

$$\langle 00 | \frac{1}{2} [\tau_a^{(1)} + \tau_a^{(2)}] | 11 \rangle = 0 , \quad (67)$$

where  $\vec{A}$  and  $\vec{B}$  are spin operators or scalar products. The index  $a$  represents the isospin of the emerging pion,  $\langle 00 |$  is the isospin state of the deuteron and  $|11\rangle$  the  $pp$  isospin initial state.

For spin,

$$\langle {}^3S_1 | \vec{S} \cdot \hat{r} | {}^3P_1 \rangle = -\sqrt{\frac{2}{3}} , \quad (68)$$

$$\langle {}^3D_1 | \vec{S} \cdot \hat{r} | {}^3P_1 \rangle = -\sqrt{\frac{1}{3}} , \quad (69)$$

$$\langle {}^3S_1 | i\vec{S} \cdot \vec{p} | {}^3P_1 \rangle = -\sqrt{\frac{2}{3}} \left( \frac{\partial}{\partial r} + \frac{2}{r} \right) , \quad (70)$$

$$\langle {}^3D_1 | i\vec{S} \cdot \vec{p} | {}^3P_1 \rangle = -\sqrt{\frac{1}{3}} \left( \frac{\partial}{\partial r} - \frac{1}{r} \right) , \quad (71)$$

$$\langle {}^3S_1 | \vec{\sigma}^{(1)} \cdot \vec{\sigma}^{(2)} i\vec{S} \cdot \vec{p} | {}^3P_1 \rangle = -\sqrt{\frac{2}{3}} \left( \frac{\partial}{\partial r} + \frac{2}{r} \right) , \quad (72)$$

$$\langle {}^3D_1 | \vec{\sigma}^{(1)} \cdot \vec{\sigma}^{(2)} i\vec{S} \cdot \vec{p} | {}^3P_1 \rangle = -\sqrt{\frac{1}{3}} \left( \frac{\partial}{\partial r} - \frac{1}{r} \right) , \quad (73)$$

$$\langle {}^3S_1 | \hat{S}_{12} i\vec{S} \cdot \vec{p} | {}^3P_1 \rangle = -2\sqrt{\frac{2}{3}} \left( \frac{\partial}{\partial r} - \frac{1}{r} \right) , \quad (74)$$

$$\langle {}^3D_1 | \hat{S}_{12} i\vec{S} \cdot \vec{p} | {}^3P_1 \rangle = -2\sqrt{\frac{1}{3}} \left( \frac{\partial}{\partial r} + \frac{5}{r} \right) . \quad (75)$$

where  $\hat{S}_{12}$  is the usual tensor operator.

## REFERENCES

- [1] H.O. Meyer *et al.*, Phys. Rev. Lett. **65**, 2846 (1990); Nucl. Phys. **A539**, 633 (1992).
- [2] D.S. Koltun and A. Reitan, Phys. Rev. **141**, 1413 (1966).
- [3] M.E. Schillaci, R.R. Silbar, and J.E. Young, Phys. Rev. **179**, 1539 (1969).
- [4] G.A. Miller and P.U. Sauer, Phys. Rev. C **44**, R1725 (1991).
- [5] J.A. Niskanen, Phys. Lett. **B289**, 227 (1992); Nucl. Phys. **A298**, 417 (1978); Phys. Rev. C **43**, 36 (1991).
- [6] T.-S.H. Lee and D.O. Riska, Phys. Rev. Lett. **70**, 2237 (1992).
- [7] C.J. Horowitz, D.K. Griegel, and H.O. Meyer, Phys. Rev. C **49**, 1337 (1994).
- [8] E. Hernández and E. Oset, Phys. Lett. **B350**, 158 (1995).
- [9] C. Hanhart, J. Haidenbauer, A. Reuber, C. Schütz and J. Speth, Phys. Lett. **B358**, 21 (1995).
- [10] S. Weinberg, Physica **96A**, 327 (1979).
- [11] J. Gasser and H. Leutwyler, Ann. Phys. **158**, 142 (1984); Nucl. Phys. **B250**, 465 (1985).
- [12] E. Jenkins and A.V. Manohar, Phys. Lett. **B255**, 558 (1991).
- [13] For a current review see V. Bernard, N. Kaiser, and U.-G. Meißner, Int. J. Mod. Phys. **E4**, 193 (1995).
- [14] S. Weinberg, Phys. Lett. **B251**, 288 (1990); Phys. Lett. **B295**, 114 (1992).
- [15] C. Ordóñez and U. van Kolck, Phys. Lett. **B291**, 459 (1992); U. van Kolck, Texas Ph.D. dissertation (1993).
- [16] C. Ordóñez, L. Ray, and U. van Kolck, Phys. Rev. Lett. **72**, 1982 (1994); Phys. Rev. C **53**, 2086 (1996).
- [17] U. van Kolck, Phys. Rev. C **49** (1994) 2932.
- [18] U. van Kolck, in *Proceedings of the Workshop on Chiral Dynamics 1997, Theory and Experiment*, ed. A. Bernstein, D. Drechsel, and T. Walcher (Springer-Verlag, 1998), hep-ph/9711222; Nucl. Phys. **A645** (1999) 273.
- [19] D. Kaplan, M.J. Savage, and M. Wise, Phys. Lett. **B424** (1998) 390; Nucl. Phys. **B534** (1998) 329.
- [20] *Nuclear Physics with Effective Field Theory*, ed. R. Seki, U. van Kolck, and M.J. Savage, World Scientific, Singapore (1998).
- [21] For a current review see U. van Kolck, Caltech preprint KRL-MAP-247, nucl-th/9902015.
- [22] T.D. Cohen, J.L. Friar, G.A. Miller and U. van Kolck, Phys. Rev. C **53**, 2661 (1996); Bull. Am. Phys. Soc. **40**, 1629 (1995), presented at the DNP/APS Fall Meeting in Bloomington, Indiana, October 1995.
- [23] U. van Kolck, G.A. Miller, and D.O. Riska, Phys. Lett. **B388**, 679 (1996).
- [24] B.-Y. Park, F. Myhrer, J.R. Morones, T. Meissner, and K. Kubodera, Phys. Rev. C **53**, 1519 (1996); T. Sato, T.-S.H. Lee, F. Myhrer, and K. Kubodera, Phys. Rev. C **56**, 1246 (1997).
- [25] C. Hanhart, J. Haidenbauer, M. Hoffmann, U.-G. Meißner, and J. Speth, Phys. Lett. **B424**, 8 (1998).
- [26] E. Gedalin, A. Moalem, and L. Razdolskaya, nucl-th/9803029; nucl-th/9812009.
- [27] V. Bernard, N. Kaiser, U.-G. Meißner, Jülich preprint FZJ-IKP-TH-1998-07, nucl-th/9806013.

- [28] V. Dmitrašinović, K. Kubodera, F. Myhrer, and T. Sato, South Carolina preprint USC-PHYS(NT)-99-03, [nucl-th/9902048](#).
- [29] G.A. Miller, F. Myhrer, T. Sato, and U. van Kolck, in progress.
- [30] V. Bernard, N. Kaiser, and U.-G. Meißner, Nucl. Phys. **A615**, 483 (1997); M. Mojžiš, Eur. Phys. J. **C2**, 181 (1998); N. Fettes, U.-G. Meißner, and S. Steininger, Nucl. Phys. **A640** (1998) 199.
- [31] V. Bernard, N. Kaiser, and U.-G. Meißner, Nucl. Phys. **B457**, 147 (1995).
- [32] J.L. Friar, D. Hüber, and U. van Kolck, Phys. Rev. C **59** (1999) 53.
- [33] C. Hanhart, talk at the INT/Argonne Workshop on Pion Production Near Threshold, Argonne National Laboratory, August 1998.
- [34] F. Mandl and T. Regge, Phys. Rev. **99**, 1478 (1955).
- [35] M. Gell-Mann and K.M. Watson, Annu. Rev. Nucl. Sci. **4**, 219 (1954).
- [36] A.H. Rosenfeld, Phys. Rev. **96**, 139 (1954).
- [37] D.A. Hutcheon *et al*, Nucl. Phys. **A535**, 618, (1991).
- [38] M. Drochner *et al*, Phys. Rev. Lett. **77**, 454 (1996).
- [39] P. Heimberg *et al*, Phys. Rev. Lett. **77**, 1012 (1996).
- [40] W.W. Daehnick *et al*, Phys. Rev. Lett. **74**, 2913 (1995); J.G. Hardie *et al*, Phys. Rev. C **56**, 20 (1997).
- [41] W.W. Daehnick *et al*, Phys. Lett. **B423**, 213 (1998); R.W. Flammang *et al*, Phys. Rev. C **58**, 916 (1998).
- [42] J.A. Niskanen, Phys. Rev. C **53**, 526 (1996).
- [43] T.-S.H. Lee, [nucl-th/9502005](#).
- [44] J.L. Friar, G.L. Payne, V.G.J. Stoks, and J.J. de Swart, Phys. Lett. **B311**, 4 (1993).
- [45] R.B. Wiringa, V.G.J. Stoks, and R. Schiavilla, Phys. Rev. C **51**, 38 (1995).
- [46] R. Machleidt, Adv. Nucl. Phys. **19**, 189 (1989).
- [47] Particle Data Group, Phys. Rev. D **50**, 1173 (1994).
- [48] T. Ericson and W. Weise, *Pions and Nuclei*, Clarendon Press, Oxford (1988).
- [49] G.A. Miller, B.M.K. Nefkens, and I. Šlaus, Phys. Rep. **194**, 1 (1990); B.M.K. Nefkens, G.A. Miller and I. Šlaus, Comm. Nucl. Part. Phys. **20**, 221 (1991).
- [50] C. Horowitz, Phys. Rev. C **48**, 2920 (1993).